Received Date : 12-Aug-2014

Revised Date : 18-Dec-2014

Accepted Date : 27-Dec-2014

Article type : Original Article

Unraveling the Peruvian Phase of the Central Andes: Stratigraphy, sedimentology and geochronology of the Salar de Atacama Basin (22°30-23°S), northern Chile

Sebastián Bascuñán[1], César Arriagada[1], Jacobus Le Roux[1, 2] and Katja Deckart[1]

[1]Departamento de Geología, Universidad de Chile, Plaza Ercilla 803, 8370450 Santiago, Chile

[2]Centro de Excelencia en Geotermia de los Andes (CEGA), Universidad de Chile, Plaza Ercilla 803, 8370450 Santiago, Chile

Corresponding author : sebascun@ing.uchile.cl

Abstract

The Salar de Atacama Basin holds important information regarding the tectonic activity, sedimentary environments and paleoclimate variations in northern Chile during Cretaceous times. About 4000 m of high-resolution stratigraphic columns of the Tonel, Purilactis and Barros Arana Formations reveal braided fluvial and alluvial facies, typical of arid to semi-arid environments, interrupted by scarce intervals with evaporitic, eolian and lacustrine sedimentation, displaying an overall coarsening-upward trend. Clast-count and point-count data evidence the progressive erosion from Mesozoic volcanic rocks to Paleozoic basement granitoids and deposits located around the Cordillera de Domeyko area, which is indicative of an unroofing process. The paleocurrent data show that the source area was located to the west. The U/Pb detrital zircon geochronological data give maximum depositional ages of 149 Ma for the base of the Tonel Formation (Agua Salada Member), and 107 Ma

This article has been accepted for publication and undergone full peer review but has not been through the copyediting, typesetting, pagination and proofreading process, which may lead to differences between this version and the Version of Record. Please cite this article as doi: 10.1111/bre.12114

for its middle member (La Escalera Member); 79 Ma for the lower Purilactis Formation (Limón Verde Member), and 73 Ma for the Barros Arana Formation. The sources of these zircons were located mainly to the west, and comprised from the Coastal Cordillera to the Precordillera. The ages and pulses record the tectonic activity during the Peruvian Phase, which can be split into two large events; an early phase, around 107 Ma, showing uplift of the Coastal Cordillera area, and a late phase around 79 Ma indicating an eastward jump of the deformation front to the Cordillera de Domeyko area. The lack of internal deformation and the thicknesses measured suggest that deposition of the units occurred in the foredeep zone of an eastward-verging basin. This sedimentation would have ended with the K-T Phase, recognized in most of northern Chile.

Keywords: Tonel Formation, Purilactis Formation, Barros Arana Formation, Salar de Atacama Basin, Peruvian Phase, braided river deposits, Chile, Central Andes

Introduction

The evolution of the Chilean Andes between 22° and 24°S (Figure 1) has been the focus of diverse studies over the last years, which have characterized the style and timing of the deformation of its different constituents (Ramírez & Gardeweg, 1982; Marinovic & Lahsen, 1984; Charrier & Reutter, 1994; Maksaev & Zentilli, 1999; Mpodozis *et al.*, 2005; Arriagada *et al.*, 2006a; Amilibia *et al*., 2008; Arriagada *et al*., 2008). These authors have shown that uplift and shortening were active during the Eocene-Early Oligocene and Neogene, although tenuous evidence of deformation during the mid- to Late Cretaceous has also been recorded. The latter event ('Peruvian Phase'; Steinman, 1929) has been identified along most of the western margin of South America (Cobbold & Rosello, 2003; Jaillard *et al*., 2005; Jaimes & De Freitas, 2006; Cobbold *et al.*, 2007; Tunik *et al.*, 2010; Martínez *et al.*, 2012, 2013), although studies concerning its effects and/or timing in the northern Central Andes are scarce.

The Salar de Atacama Basin, located to the east of the Precordillera (known locally as the Cordillera de Domeyko) (Figure 1, Figure 2), has an important geological record from mid-Cretaceous to present times (Brüggen, 1934, 1942, 1950; Charrier & Muñoz, 1994; Charrier & Reutter, 1990, 1994; Arriagada, 1999; Mpodozis *et al.*, 2005; Arriagada *et al*., 2006a). Even though much work has been done with regard to its stratigraphy, sedimentology (Brüggen, 1942; Dingman, 1963, 1967; Hartley *et al.*, 1988, 1992) and structure (Macellari *et al.*, 1991; Muñoz *et al*., 2002; Arriagada, 1999; Pananont *et al.*, 2004; Mpodozis *et al*., 2005; Arriagada *et al*., 2006a; Reutter *et al.*, 2006), the Tonel, Purilactis and Barros Arana Formations (which constitute the Purilactis Group *sensu* Mpodozis *et al.*, 2005) still

pose important questions about their origin, tectonic setting(s) and, inextricably, about the uplift of the Cordillera de Domeyko during the Late Cretaceous. The lack of fossils, tuff layers or other stratigraphic indicators has made dating of these units problematic; the only ages available have been obtained through Ar-Ar analysis of weathered samples (Flint *et al.*, 1989) and in samples south of the Barros Arana Syncline, from Maastrichtian or younger units (Ramírez & Gardeweg, 1982; Hammerschmidt *et al.*, 1992; Charrier & Reutter, 1990, 1994; Arriagada, 1999; Mpodozis *et al.*, 2005); additionally, no dating of samples belonging to the Tonel Formation has been performed. Thus, the time span of these formations remains poorly constrained.

In this contribution, we measured almost 4000 m of high-resolution stratigraphic sections in the Purilactis Group, in order to establish the relationship between the depositional environments and concomitant tectonic pulses. This, in turn, aids in clarifying the tectonic setting prevalent from Late Cretaceous to Paleogene times. Additionally, eleven samples were taken for provenance analysis, of which eight were selected for LA-IPC-MS U-Pb detrital zircon geochronological dating, in order to better constrain the age and provenance of the Purilactis Group.

Geological setting

The Salar de Atacama Basin is one of the most recognizable topographic features in the Chilean Central Andes (Figure 1) (Isacks, 1988; Allmendinger *et al*., 1997; Jordan *et al*., 2002; Götze & Krause, 2002; Yuan *et al*., 2002; Arriagada *et al*., 2006a). It is located between 22°30'S and 24°30'S, being a 150 km long (N-S) and 80 km wide (E-W) oriented depression, with its lowest point at 2300 m a.s.l. It lies immediately to the east of the Precordillera and west of the magmatic arc, whose axis shows a 60 km displacement to the east relative to the rest of the arc.

The Precordillera/Cordillera de Domeyko is a well-defined morphostructural unit about 500 km long (N-S), divided into different units formed by a series of basement structures, whose cores are composed of basement rocks bounded by high-angle faults (Amilibia *et al*., 2008). In the Salar de Atacama area, the Cordillera de Domeyko reaches ~3000 m a.s.l. and consists of Paleozoic to Mesozoic ignimbritic and rhyolitic successions associated with basaltic and andesitic rocks, intruded by granitoids with ages spanning between 200-300 Ma (Breitkreutz & Van Schmus, 1996; Arriagada *et al*., 2006a). Evidence of widespread exhumation during the Eocene, possibly related to the Incaic Event, has been previously described (Ramírez & Gardeweg, 1982; Charrier & Reutter, 1994; Maksaev & Zentilli, 1999; Charrier *et al.*, 2009), although syntectonic structures found in Cretaceous

successions point to an even earlier event of uplift and erosion (Mpodozis *et al*., 2005; Arriagada *et al*., 2006a; Amilibia *et al*., 2008). The eastern limit of the range coincides with the El Bordo Escarpment (Figure 2), which exhibits outcrops of Mesozoic and Cenozoic rocks (Charrier & Muñoz, 1994; Arriagada, 1999; Mpodozis *et al*., 2005; Figure 2 in Arriagada *et al*., 2006a). To the NNE, between 22°30'-23°S, the Mesozoic formations are folded into the Barros Arana Syncline, which is 80 km long (NE-SW) and 16 km wide (NW-SE) (Hartley *et al*., 1988, 1992; Arriagada, 1999; Mpodozis *et al*., 2005; Arriagada *et al*., 2006a).

East of the El Bordo Escarpment lies the Llano de la Paciencia, a sub-basin 80 km long (N-S) and 8 km wide (E-W), which is filled primarily by Quaternary alluvial fans (Marinovic & Lahsen, 1984; Jolley *et al*., 1990; Arriagada, 1999; Mpodozis *et al*., 2005). To the east, the Cordillera de la Sal, a SSW-NNE structure 5 to 10 km wide, reaches ~200 m above the basin floor, where Oligocene to Pliocene evaporate-rich sedimentary units are folded (Flint *et al*., 1993; Jordan *et al*., 2002; Arriagada *et al*., 2006a). The present salt pan (salar), formed by a Quaternary alluvial and evaporitic fill, is located east of the Cordillera de la Sal, and overlies Cretaceous to Neogene rocks (Ramírez & Gardeweg, 1982; Marinovic & Lahsen, 1984; Macellari *et al*., 1991; Muñoz *et al*., 1997; Jordan *et al*., 2002; Lowenstein *et al*., 2003; Arriagada *et al*., 2006a) .

The basin shows outcrops of ignimbritic successions of Miocene and Pleistocene age towards its eastern border, which corresponds to the current magmatic arc and its deposits (Ramírez & Gardeweg, 1982; Marinovic & Lahsen, 1984). The basin is bounded to the south by the Western Cordillera (Arriagada, 1999; Arriagada *et al.*, 2006a) and the Cordón de Lila Range, composed of igneous and sedimentary rocks of Ordovician-Carboniferous age (Niemeyer, 1989; Coira *et al*., 2009).

Cretaceous rocks in the Salar de Atacama Basin consist of the Purilactis Group (Figures 3, 4, 5 and Table 1) (*sensu* Mpodozis *et al*., 2005), which contains the Tonel, Purilactis, Barros Arana and Cerro Totola Formations.

The Tonel Formation is divided into three members (Arriagada, 1999; Mpodozis *et al*., 2005), starting with ~60 m of basal breccias and pebble conglomerates with andesitic, rhyolitic and sedimentary clasts (Mpodozis *et al*., 2005), deposited in the proximal parts of alluvial fans and valley-fills (Hartley *et al*., 1992). The middle member is composed of 400 to 1000 m of brown to red, horizontally

laminated sandstones, at times alternating with gypsum layers, followed by a top member of unknown thickness containing deformed anhydrite deposits. The last two members display paleocurrent directions, such as planar-cross bedding in sandstones, indicating a western provenance (Mpodozis *et al*., 2005), and the depositional setting is interpreted as a playa-lake or continental sabkha environment (Hartley *et al*., 1992). The contact between the Tonel and Purilactis Formations is frequently faulted (detached) (Figure 6) (Hartley *et al*., 1988; Arriagada, 1999; Mpodozis *et al*., 2005; Arriagada *et al*., 2006a).

The Purilactis Formation has five members reaching a total thickness of about 3000 m according to Hartley *et al*. (1992) and subsequent researchers (*e.g.* Arriagada, 1999; Mpodozis *et al*., 2005; Arriagada *et al*., 2006a). The basal portion is represented by the Limón Verde Member, containing 420 m of sandstones and brownish-reddish conglomerates, interpreted as proximal alluvial fan deposits, grading into fine playa-lake deposits towards its upper 40 m, where it shows the transition into the Licán Member (Hartley *et al*., 1992; Arriagada, 1999; Mpodozis *et al*., 2005). The latter contains about 700 m of sandstones and red mudstones, interbedded with conglomerates and evaporites, which are interpreted as representing channelized medial to proximal fluvial deposits with distal sheetfloods and playa-lakes (Hartley *et al*., 1988, 1992; Arriagada, 1999). The Vizcachita Member overlies the Licán Member with a sharp contact, displaying predominantly eolian facies, with a greater percentage of fluvially reworked deposits in the western outcrops, while finer-grained eolian sandsheets and barchans up to 30 m high dominate the eastern deposits. The fluvial sections show a western provenance, while the dunes indicate paleocurrent directions from the south (Hartley *et al.*, 1992; Arriagada, 1999). The change to an eolian facies may be due to a cessation of tectonic activity, which would have starved the basin of a fluvial input until deposition of the Seilao Member (Hartley *et al.*, 1992). Andesitic flows are found in some locations at the contact between the Vizcachita and Seilao Members (Quebrada Seilao, Hartley *et al*., 1988, 1992). The Seilao Member shows a return to predominantly alluvial facies, with the presence of poorly confined conglomeratic sheetflood and high-density flood deposits. Some fluvial deposits can be found as small-scale, fining-upward cycles (Hartley *et al.*, 1992; Hartley, 1993), probably representing meandering streams. The Seilao Member fines upward into the 250 m thick Río Grande Member, which contains sandstones, siltstones and varved mudstones, evidencing a possibly permanent, shallow lake subject to alluvial flooding and deposition of distal sheetflood sands (Hartley *et al.*, 1988, 1992; Arriagada, 1999).

The Río Grande Member represents the last unit of the Purilactis Formation, conformably underlying the Barros Arana Formation (Arriagada, 1999). According to Hartley *et al.* (1992), the latter is composed of thick alluvial fan deposits with clasts up to 20 cm in diameter, derived mostly from

Paleozoic granitoids and rhyolites with minor andesites and limestones in the west. The dominant facies are laterally amalgamated, proximal channelized streamflow and sheetflood deposits, together with some high-density flood and debris flow deposits. The large amount of basement-derived clasts, as compared to the Purilactis Formation, suggests deep exhumation of the Cordillera de Domeyko Range during its deposition (Mpodozis *et al.,* 2005).

The Purilactis Group (*sensu* Arriagada, 1999) ends with the Cerro Totola Formation ('Estratos Cerros de Totola' of Arriagada, 1999 and Mpodozis *et al.*, 1999), which is mainly composed of andesites, basaltic andesites and fewer dacites, interbedded with welded rhyolitic tuffs and some sandstones and red volcaniclastic conglomerates (Arriagada, 1999). This unit unconformably overlies deposits of the Tonel Formation and the Licán Member and is currently interpreted as younger than the Barros Arana Formation (Arriagada, 1999; Mpodozis *et al.,* 1999, 2005).

Regarding the age, lavas and related intrusives belonging to the Cerro Totola Formation, which intrude both the Tonel and Purilactis Formations, present K-Ar ages ranging between 70.2±2.0 and 61.0±2.0 Ma, within the Maastrichtian – Danian range, defining a minimum age for the lower terms of the Purilactis Group (Mpodozis *et al.,* 2005). This age is in agreement with a K/Ar age of 63.6±2.8 Ma obtained by Macellari *et al.* (1991) from similar hornblende-rich dykes that intrude the lower Tonel Formation. The maximum age of the group has not been conclusively determined; paleomagnetic studies of the middle member of the Tonel Formation and the Limón Verde and Licán Members of the Purilactis Formation show that these rocks acquired their magnetization during a period of normal polarity, suggesting deposition during the Cretaceous normal polarity superchron (119-84 Ma) (Arriagada, 1999; Arriagada *et al.,* 2000). In addition, Ramírez and Gardeweg (1982) found reworked limestone clasts in the Purilactis Formation containing pelecypods (*Vaugonia v. l. gottschei* Moericke) and ammonites (*Perisphinctes* sp.,) of Middle Jurassic age, which confirms a post-Jurassic age for the group (Mpodozis *et al.,* 2005).

Sedimentology

Stratigraphic columns, measured on a centimeter to meter scale, and lithological information were collected from different sections throughout the Barros Arana Syncline (Figures 2 and 3). Conglomerate clast counts were performed on at least 100 clasts inside a 50x50 cm grid in selected areas, and paleocurrent directions were measured using paleochannels, troughs and/or lee side laminae, following method II of DeCelles *et al.* (1983). The clast count and paleocurrent information

were then compared with data previously published by Hartley *et al.* (1988, 1992). The facies code used here (Table 2; Figures 4 and 5) is partly modified from Miall (1996), Nalpas *et al.* (2008), Carrapa *et al.* (2012), Siks and Horton (2011) and DeCelles *et al.* (2011). Sedimentological analysis and depositional environment interpretation are based both on the data acquired in this research and that of Hartley *et al.* (1988, 1992), Arriagada (1999) and Mpodozis *et al.* (2005). The more detailed columns can be seen in Supplementary Material A. The subdivisions for the formations proposed by Henríquez *et al.* (in prep.) are used here.

Lithofacies Assemblages

Due to the large amount of columns profiled in this study, and in order to avoid excessive detail, we describe only the main lithofacies assemblages identified in the Barros Arana Syncline. These correspond to:

(a) Shallow, gravel-bed, braided rivers: This assemblage consists mainly of crudely stratified and/or massive, clast-supported conglomerates (Gch and Gcm, respectively), with clast sizes usually in the granule-pebble range, containing at times isolated clasts of larger sizes (up to 40 cm). The clasts are usually poorly sorted and subrounded to angular in shape, while the matrix is composed of a poorly sorted, subangular, coarse- to very coarse-grained sandstone. The most common colors are usually variations of brownish red to brown, and on some occasions grey. Bed thicknesses vary from member to formation, but they are usually between 15 cm to 1 m, forming compound units 5 to 15 m thick; the overall low thickness of these beds suggests unchannelized flooding on the lower reaches of alluvial fans (Nemec & Steel, 1984). The individual beds may be hard to identify sometimes, and the contacts between lithosomes are usually slightly erosive, and they may show a fining-upward trend. These conglomerates are generally tabular, though they sometimes show lenses a few cm thick and a meter or so wide, containing matrix-supported conglomerates (either Gmm or Gcm); the tabular character of the beds suggests unconfined or poorly confined flows able to spread laterally while depositing poorly sorted and slightly organized facies ("Sheet Gravels" of Harvey, 1984). This lithofacies is usually intercalated with laminated and horizontally stratified sandstones (Sh and Sl). This pattern of stratified conglomerates interbedded with laminated sandstones is a common sight in braided stream conglomerates, where slight fluctuations in stream velocity may produce this alternation (Nemec & Steel, 1984). Some minor gravity-flow deposits, usually ocurring with this assemblage, have been identified; they are distinguished by a larger presence of massive, matrix- and clast-supported conglomerates (Gmm and Gcm, respectively), which may also show fining- and coarsening-upward trends. Basal contacts are usually sharp and non-erosive, though they might appear irregular when the

sediment is deposited over an eroded surface. The lithosomes may be up to 8 m thick. Even though it is considered part of a different assemblage by Miall (1996) we include it here due to its minor occurrence.

(b) Deep, gravel-bed, braided rivers: This assemblage is recognized by the presence of fining-upward cycles, 6 to 30 m thick, containing either a stratified or massive basal conglomerate (Gch or Gcm) showing basal scouring, slight channelization, poor to regular sorting and subangular, cobble-to pebble-sized clasts, followed by clast-supported conglomerate bodies around 1 m thick interbedded with medium-to very coarse-grained sandstones. This indicates the development of cycles in channels more than 1 m deep (Miall, 1996). The contacts between these lithosomes are non-erosive and diffuse. The sandstone portion varies from scarce to more than half of an individual cycle. The conglomerates are mostly stratified (Gch), or massive (Gcm) with clast sizes mostly in the granule-pebble range, though they can be cobble-sized locally. The conglomerates can contain boulders up to 40 cm in diameter; this is a common sight in comparison to the previous assemblage. The cycles end with coarse- to medium-grained, laminated sandstones (Sl) containing isolated clasts, with the top usually eroded by the subsequent cycle. Planar, cross-stratified conglomerates (Gpt) may also be found, though not commonly. The colors observed are usually brownish red to different shades of grey.

(c) Distal, sheetflood, sand-bed river: This style of sand-bed rivers is one of the most ubiquitous assemblages identified in the field, together with (a). It is comprised of horizontally laminated sandstones, both very fine- to medium-grained (Sh) and medium- to very coarse-grained (Sl); this lamination may locally become very faint. Sorting varies from good to poor, especially when they are found close to conglomerates or coarser-grained deposits, and roundness is usually subangular to subrounded. The lithosomes may have isolated clasts up to 30 cm in diameter, and may also fine upward; they are, characteristically, tabular in shape, with no apparent channelization. Bed sizes are usually between 15 to 50 cm thick, although coarser-grained facies may be thicker on rare occasions (up to 8 m). Contacts are usually sharp and non-erosive. They can also show clast-supported conglomerate lenses with granule- to pebble-sized clasts, presenting basal scouring (either Gcm or Gch). Sandstones with trough cross-bedding (St) may be locally found, as lithosomes usually thicker than the other sandstone lithofacies (between 1 to 6 m thick). They present the widest variety of colors of all assemblages.

(d) Eolian deposits: This assemblage comprises homogeneous, grey, medium- to fine-grained sandstones with horizontal lamination (Sh), good sorting and subrounded grains. It shows practically no variations throughout most of the measured section, except for sparse outcrops of poorly sorted, brown, coarse-grained sandstone (Sl) with isolated clasts up to 5 cm in diameter. Lamination is faint in some instances; in higher parts of the column, both horizontal bedding and cross-lamination are clearly developed, showing beds around 30 cm thick. These lithofacies are closely associated with large-scale cross-stratified sandstones (St) (Figure 5e), which show no evident change in textural maturity or composition. The lithosomes are up to 25 m thick. These deposits have been identified as eolian deposits (Kocurek 1981, 1991), consisting of fluvially reworked eolian sandstones, eolian dunes and sandsheets. The dunes have been previously identified as barchans by Hartley *et al.*, (1988; 1992).

(e) Lacustrine deposits: The abundant occurrence of fine- to very fine-grained sandstones (Sh) and siltstone beds (Fm), usually green or dark brown in color, marks the presence of this assemblage. The former beds are characteristically either dark green or dark brown, while the latter are usually yellowish. Beds are usually less than 50 cm thick, and may fine upward. They are usually covered or only partially exposed in the sections studied. It is also common to find minor lenses of clast-supported conglomerate lenses (Gcm) and coarse-grained, laminated sandstones (Sl).

Stratigraphic distribution of lithofacies assemblages

The distribution of the assemblages during the Cretaceous is as follows:

Tonel Formation

The lowermost division of the Tonel Formation corresponds to the Agua Salada Member, which was studied in the northwestern part of the Barros Arana Syncline (Figure 2), where it overlies andesitic and tuffaceous rocks of the Tuina Formation (Raczynski, 1963; Henríquez *et al.*, in prep.) with a slight angular unconformity. Here, this member (Figure 7a and A.1) is composed of ca. 168 m of light brown deposits of shallow, gravel-bed, braided rivers. A conformable, non-erosive contact with laminated sandstones at ca. 168 m of the same section (Figure 7a and A.2) marks the limit with the La Escalera Member, which shows a transition to a more distal environment, with the presence of sheetflood, sand-bed river deposits of a reddish brown color (Figure 5a). At ca. 230 m, the outcrops are partly covered and darker in color, representing intervals of the same sand-bed river deposits interbedded with scarce lacustrine assemblages. No outcrops are present above ca. 322 m. This member is followed by the Arcoiris Member, which is the top of the Tonel Formation; it was not

measured in this study. It lies below the Purilactis Formation (Los Cóndores Member), showing a marked detachment in the southern part of the syncline (Figure 6a), where it is composed of intercalated siltstones, fine-grained orange sandstones and light-grey evaporites (gypsum and halite) (Hartley *et al.*, 1988, 1992; Arriagada, 1999; Mpodozis *et al.*, 2005; Henríquez *et al.*, in prep.). Due to its intensely-folded structure, its thickness is hard to determine, though it ranges between 50 and 300 m.

Purilactis Formation

The Los Cóndores Member (Figure 3), not measured in this study, corresponds to the first member of the Purilactis Formation (basal section of the Limón Verde Member *sensu* Arriagada, 1999; upper part of the Tonel Formation *sensu* Hartley *et al.*, 1992). The nature of the contact changes throughout the syncline; to the north, the contact is conformable with the Tonel Formation, as clearly seen on satellite images, while, to the south, it is detached (Figure 6a). According to Arriagada (1999), it comprises ca. 320 m of reddish brown lithofacies belonging to distal, sheetflood, sand bed-rivers with a high braiding index, which is characteristic of distal braid plains. It is overlain in sharp but conformable contact by the Limón Verde Member, showing a sharp contact between them (Figure 6b), where an important change in color is observed. The basal section of this member, studied in the western limb of the syncline (Figure 7b and A.3), shows grey to green deposits of distal, sand-bed rivers, which become more reddish towards the top (up to ca. 414 m) (Figure 5b). They also show an overall coarser profile. At ca. 414 m, the lithofacies assemblages and the development of different cycles indicate a transition to deep, gravel-bed braided rivers until ca. 708 m. From this point onwards, there is a return to sandy, sheetflood assemblages until ca. 936 m, where the deposits grade into brownish sandstones and conglomerates of the Lampallar Member. The contact between both units is more clearly appreciated in the field in the southern portions of the syncline, where it rests conformably on the Limón Verde Member (Figure 2). It is the first of the subdivisions for the Licán Member (*sensu* Hartley *et al.*, 1992) proposed by Henríquez *et al.* (in prep). The Lampallar Member (Figure 7c and A.4) shows 250 m of brown to dark brown lithofacies of shallow, gravel braided rivers (Figure 5c), with scarce gravity flow intercalations, as shown by the presence of sparse matrix-supported conglomerates. Similar assemblages are found upwards, in the Licán Member, observed in the same flank (Figure 2). It shows a gradual transition from the previous member (Figure 7d and A.5), where a change to red sandstones marks the difference between both units (Figure 5d). The interpretation for this member is quite similar to the one given for the Lampallar Member, though with a fining-upward trend. More reddish beds could also indicate increased subaerial exposure, which is also reflected by the presence of burrows toward the top of the section. Also, gravity flow deposits are scarcer than in the previous member. The Licán Member is overlain by the Pajarito Member, observed in the western

flank of the syncline, where it conformably underlies the Vizcachita Member (Figure 6c). The Pajarito Member (Figure 7e and A.6) shows brown to reddish brown sandstones and conglomerates, grading from reddish sandstones of the previous subdivision. The column profiled shows, in its first 78 m, lithofacies belonging to gravel-bed, probably shallow rivers, with a channel depth of ca. 1 m, while the upper portion (until ca. 105 m) signals a change to ephemeral sheetflood, sand-bed rivers.

The Vizcachita Member was partly observed in the northeastern section of the Barros Arana Syncline (Figure 7f and A.7). It shows a transitional contact with the Pajarito Member (Figure 6c); though the color clearly changes on satellite images, similar facies are found in both members near their contact. The deposits observed in the ca. 205 m column are characteristic of eolian deposits (Figure 5e) and ephemeral sand-bed rivers. Hartley *et al.* (1988) suggest a fluvial origin for some of these sandstones, although they also note that this member presents strong lateral variations into eolian dunes and eolian sand sheets. They also show that the eastern flank of the syncline presents a more abundant proportion of eolian sandsheets and dunes than the western flank, which is interpreted to have had a more important fluvial input. This member also presents an andesitic intercalation towards its top, in some places, marking the contact with the Seilao Member (Hartley *et al*., 1992; Arriagada, 1999).

The Seilao Member (Figure 7g and A.8), studied on the western flank of the syncline, shows a return to coarser facies, presenting ca. 594 m of brown, shallow, gravel-bed braided river deposits, with intervals dominated by ephemeral sheetflood deposits (coarse-grained, laminated sandstones (Sl)) (Figure 5f). A change to finer-grained lithofacies characterizes the deposits of the Río Grande Member, partly observed above the section described for the Seilao Member (Figure 7h and A.9). The contact between members is sharp, conformable, and traceable on satellite images (Figure 2). The section shows ca. 85 m of brown to green lithofacies related to ephemeral, poorly confined sand-bed rivers, and possibly lacustrine deposits. The outcrops are mostly covered towards the top.

Barros Arana Formation

The Barros Arana Formation was studied in a section directly east of the one described for the Río Grande Member (Figure 7i and A.10), where it forms the core of the Barros Arana Syncline. The section starts with ca. 182 m of green to brown deposits resembling both the distal sand-bed river and shallow, braided river assemblages (Figure 5g), with a slight dominance of the former. At ca. 182 m, the column is dominated by assemblages of deep, gravel-bed braided rivers, with lesser intercalations of distal, sheetflood deposits; these deposits are no more than 30 m thick at a time, and usually exhibit

a more reddish color. The column profiled is quite homogeneous until its end at ca. 928 m, where it reaches the axis of the syncline.

Paleocurrent data

Data for paleocurrent analysis were obtained primarily from paleochannels and parting lineations found throughout the study area (Figure 3 and 8 and Supplementary Material A); in the case of scalars, the direction assumed was the same as that of the closest vectors obtained from other structures, like imbricated clast orientations, planar cross stratification and 3-D expositions of trough cross-strata. These measurements were taken in the Agua Salada and La Escalera Members of the Tonel Formation, the Limón Verde, Lampallar, Licán, Pajarito (the last three grouped together), Vizcachita and Seilao Members of the Purilactis Formation, and the Barros Arana Formation. The data was then tilt-corrected with ROTDIR (Le Roux, 1991) and restored to their original orientation by rotating them 30° counterclock-wise, following various paleomagnetic studies that show such an amount of clockwise rotations in the forearc area during the Tertiary (Arriagada *et al.*, 2000, 2003, 2006b). The corrected data show that the Tonel Formation presents paleocurrents indicating a predominantly NNE flow, and fewer paleocurrents in the NW and ESE directions. The Limón Verde Member presents one main paleocurrent direction showing paleochannels and parting lineations towards the ESE, and another group of indicators pointing towards the NE. The Lampallar, Licán and Pajarito Members show a dominant transport to the E, recorded in many cross-stratified sandstones, with only a few structures pointing towards the NW. The Vizcachita Member presents large paleodunes indicating sediment transport to the WSW (Figure 5e). Data from the Seilao Member show a clear ESE tendency, with some structures pointing to the ENE. The Barros Arana Formation shows a major component to the NE, and a second one to the WNW; the latter component could possibly reflect diagonal and/or point bar migration (Hein, 1984).

This information indicates a general west to east (NE-ESE) transport in most formations and members, with the exception of the mainly eolian Vizcachita Member showing westerly transport, which is consistent with measurements taken by Hartley *et al.* (1988, 1992). This preferred easterly to southeasterly direction is likely due to uplift of the Cordillera de Domeyko Range (Figures 1 and 2), situated west of the study location, during the sedimentation of the three formations. In this regard, Mpodozis *et al.* (2005) and Arriagada *et al.* (2006a) found growth structures in strata belonging to the Tonel Formation, which indicate a compressional regime during their sedimentation in mid-Cretaceous times; the space available for sediment accumulation and the deformation observed would be partly due to an eastward-verging thrust system related to the Cordillera de Domeyko Range. The

directions observed in the Vizcachita Member attest to the main wind direction during its deposition (Kocurek, 1981, 1991). Hartley *et al.* (1992) obtained paleowind directions to the north; this discrepancy could result from the interpretation of the structures observed in this member (Figure 5e), where they could be either classified as tangential cross-laminated sets or one flank of a large trough formed by a barchan dune.

Provenance

Conglomerate clast count

Clast counts were performed on the Tonel Formation (Agua Salada Member), the Limón Verde, Pajarito and Seilao Members of the Purilactis Formation and the Barros Arana Formation (Figure 9). The Agua Salada Member shows a predominance of andesitic and tuffaceous clasts, with only 10% of clasts being of sedimentary rock origin. These are, most likely, a product of erosion within the same formation. The Limón Verde Member presents andesitic clasts as its key component, together with only a minor proportion of sedimentary clasts (15-20%), and even fewer rhyolitic to dacitic tuff clasts (less than 10%). The observed siltstone and sandstone clasts are similar to the facies described for this member, making them a product of limited erosion or cannibalism. The Lampallar and Licán Members (only qualitatively observed) show clasts of andesitic composition (more than 90%), with few sandstone clasts in the former, while the Pajarito Member shows rhyolitic to dacitic tuff clasts (80%) together with andesitic clasts (18%). The Seilao Member shows a prevalence of andesitic clasts, followed by granitic clasts, in a 3:1 ratio; this is reversed towards the top of the section. Finally, the Barros Arana Formation shows an increasing proportion of granitic vs. andesitic clasts (around 80% for the former and 20% for the latter), with only minor sandstone and limestone clasts (less than 5%).

The sections observed document an abundant presence of andesitic clasts, and a gradual increase of granitic, coarse-grained clasts over time; this is most evident in the Barros Arana Formation and Seilao Member sections, where granitic boulders can exceed 30 cm in diameter. These clasts are derived from granitoids probably representing deep exhumation of the Cordillera de Domeyko area (Mpodozis *et al.*, 2005; Basso & Mpodozis, 2012). The source of the andesitic clasts is most likely the Tuina Formation (Raczynski, 1963) and/or exhumed levels of the Late Cretaceous-Eocene Arc (Hartley *et al.*, 1992).

Hartley *et al.* (1988, 1992) obtained similar clast compositions, with a higher percentage of limestone clasts in the Purilactis Formation; this is attributed to uplift of the Triassic-Lower Cretaceous back-arc basin fill, due west of the study area, which is consistent with observed paleocurrent bearings and growth structures (see above).

Sediment provenance

Provenance analyses were performed on 11 medium- to coarse-grained sandstones. Of these, one was taken from the Tonel Formation (La Escalera Member), nine from the Purilactis Formation and one from the Barros Arana Formation. Around 400 to 500 grains exceeding 0.0625 mm in diameter were counted using a Swift point counter, following the Gazzi-Dickinson method (Dickinson, 1970; Dickinson & Suczek, 1979; Dickinson *et al*., 1983; Ingersoll *et al*., 1984; Dickinson, 1985). The parameters and point-counting raw data are listed in Table 3 and Supplementary Material B. The results were plotted on different ternary diagrams, following Dickinson (1985), Weltje (2006) and Ingersoll (2012), and partly using an electronic spreadsheet developed by Zahid & Barbeau (2011) (Figure 10). The geometric mean was calculated for the Purilactis Formation, following the reasoning provided by Weltje (2002).

The La Escalera Member and the basal Limón Verde Member samples show an important amount of plagioclase, K-feldspar and quartz over lithic fragments; the quartz observed is mostly monocrystalline, while lithics are mostly andesitic, microlithic fragments. Samples collected higher in the stratigraphic record (upper Limón Verde Member and samples of the Licán Member *sensu* Hartley *et al.*, 1992) show a more important presence of lithic fragments and plagioclase, occasionally containing red siltstone and minor quartz-feldspathic sandstone fragments. The sandstones of the Vizcachita Member show an overall lower percentage of quartz relative to other components, and a relevant presence of andesite fragments; plagioclase and quartz are again important in the Seilao Member, the latter being less abundant in the Río Grande Member. The geometric mean of the Purilactis Formation shows that plagioclase is the most important constituent, followed by monocrystalline quartz, lithic fragments and K-feldspar. Finally, the Barros Arana Formation sample shows monocrystalline quartz and plagioclase as major components. Some accessory minerals found throughout the section comprise iron oxides and micas, hornblende and, in some cases, broken, almost fresh pyroxene, particularly in the samples belonging to the Río Grande and Vizcachita Members.

Most of the sandstones collected plot between the basement uplift and transitional to dissected arc fields though some samples may show some divergence when different diagrams are used. No clear temporal trend can be observed, though the two upper formations plot closer to the volcanic arc fields, particularly the dissected to transitional arcs in the case of the Barros Arana and Purilactis Formations (Figure 10, a, b). The La Escalera Member plots clearly in the basement uplift field, which is the product of the erosion of uplifted, deeply incised basement; however, Dickinson *et al.* (1983) concede that volcanic arcs can show similar compositions if they are intensively dissected, so that petrographic methods do not help in clarifying the tectonic regime if compositional overlap occurs. In this regard, the petrographic classification must only be seen as a first-order classification.

Weltje (2006) tested the model proposed by the aforementioned authors, and produced modified ternary diagrams by means of statistical analysis. The diagrams are partitioned into three spaces separated by iso-density probability lines, where the grand means of each provenance association and their confidence regions are plotted. The efficiency of the partitioning and the predictive utility of these new diagrams were tested by stochastic simulations. The results show that probabilities of correct inference are: QpLvLs (78%), QFL (76%), QmFLt (74%) and QmPK (64%) (Figure 10, c, d, e, f). Also, Ingersoll (2012), who worked on the Sierra Nevada and Southern Cascade Magmatic Arc proposed a QpLvFp diagram (Figure 10g) based on the discriminant analysis of modern sands shed from the arc. The latter shows a N-S trend, with more exhumation toward its southern end (basement uplift) than the north (undissected arc).

Following these diagrams (Figure 10, c, d, e, f), the Tonel Formation falls in the basement uplift and continental block fields, with only one diagram (Figure 10f) showing a different field. The Purilactis Formation, as a whole, plots in the magmatic arc field, though very close to the continental block field, while the Barros Arana Formation plots mostly in the continental block field. On the QpLvFp diagram (Figure 10g), the sandstones of the Purilactis and Barros Arana Formations are located between the transitional and dissected arc fields, while the Tonel Formation is found between the recycled orogen and dissected arc fields.

U-Pb Detrital geochronology

Due to the lack of beds and deposits suitable for more detailed geochronology studies, such as tuffs or other extrusives, U-Pb detrital geochronological analyses by means of laser ablation-multicollector-inductively coupled mass spectrometry were used to constrain the age of these deposits. A total of

eight, fine- to coarse-grained samples, encompassing all the formations studied, were chosen for analysis; these were taken from the Tuina area and the Barros Arana Syncline (Figure 2).

Zircon separation was performed at the Sample Preparation Laboratory (Laboratorio de Preparación de Muestras) of the Universidad de Chile using the Gemeni table, Frantz magnetic separator and heavy liquid procedures. They were then manually separated from other minerals using a binocular microscope. The zircon mineral separates were sent to the Laboratorio de Estudios Isotópicos (LEI), Geoscience Center, Universidad Nacional Autónoma de México (UNAM), Mexico, where around 100 randomly chosen grains were analyzed. The analytical work was undertaken by using a *Resonetics Resolution M50* 193 nm laser *Excimer* connected to a *Thermo Xii Series Quadrupole Mass Spectrometer* following analytical procedures and technical details after Solari *et al.* (2010). The employed laser diameter for ablation was 23 μm, and the analysis was performed randomly on the grain surface. The best age was defined using the $^{206}Pb/^{238}U$ and $^{207}Pb/^{206}Pb$ ratios, with an 800 Ma cutoff. Average ages were calculated using *Isoplot v. 3.7* (Ludwig, 2008); they represent the youngest populations ($n \geq 3$) for each of the eight analyzed zircon samples. The maximum depositional age for each sample locality is given by this age. Age peaks and populations were also calculated using the Excel spreadsheet Age Pick, provided by the LaserChron Center at the University of Arizona. The Excel spreadsheet Normalized Age Probability Plots, also provided by the University of Arizona, was used to summarize the relative probability plots of the different samples. The results can be seen in Figure 11. The data tables are shown in Supplementary Material C.

Tonel Formation

Samples from the Tonel Formation (Figure 11a-c) show contrasting age populations. The basal sample is SP1-15, taken from the Agua Salada Member (Figure 2, Figure 11a). It presents most of its zircons (n = 28) around 247 Ma (Permian-Triassic); other important populations are in the Ordovician (n = 5 around 472 Ma and n = 4 around 483 Ma), the Permian (n = 5 around 279 Ma) and the Permian-Carboniferous (n = 3 around 302 Ma). A minor population around 149 Ma (n = 3, latest Jurassic) defines the maximum depositional age for the sample. The relative probability plot shows its most important peak at 247 Ma, followed by a minor peak at 149 Ma.

Sample K-4 (Figure 11b), taken from the La Escalera Member, close to the contact with the Agua Salada Member, presents n = 24 zircons in the Triassic, with n = 5 zircons around 211 Ma, n = 7 around 219 Ma and n = 12 around 230 Ma. These are followed by Permian-Triassic (252 Ma, n = 19),

Permian-Carboniferous (n = 8 around 291 Ma and n = 7 around 299 Ma), mid- to Early Cretaceous (n = 5, around 107 Ma), Jurassic (153 Ma, n = 4) and Permian (275 Ma, n = 3) populations. The mean age obtained for the youngest population is 107 Ma, which corresponds to the maximum depositional age of the sediment. The relative probability plot shows a high age peak around 252 Ma, followed by 230 Ma and 107 Ma peaks.

Sample K-18, taken from the Arcoiris Member (Figure 11c) presents a maximum depositional age of 141 Ma. The largest populations found are of Ordovician (n = 4 around 459 Ma and n = 7 around 480 Ma) and Ediacaran (n = 6 around 566 Ma and n = 4 around 590 Ma) age. Other noteworthy populations are found (in decreasing order) in the Triassic (n = 5 around 228 Ma and n = 4 around 243), the Cambrian (566 Ma, n = 6), Permian-Carboniferous (n = 6 around 303 Ma), the Permian (260 Ma, n = 5), and the Early Cretaceous (142 Ma, n = 5). It is also worth noting that this sample has zircons in the Meso-Proterozoic (1000-1600 Ma), with n = 10 around 1125 Ma. The relative probability plot shows its most prominent peaks around 142 Ma and 228 Ma.

Purilactis Formation

Limón Verde Member

The Limón Verde Member samples, taken near the Cordón de Barros Arana (Figure 2), show similar ages, but present varying proportions of older zircons. The basal sample (SP3-90, Figure 11d) presents an important population (n = 13) around 81 Ma (Late Cretaceous); the maximum depositional age is 79 Ma. The second most important population is located in the Cambrian (n = 4 around 524 Ma and n = 5 around 538 Ma), followed by the Ordovician (n = 3 around 466 Ma and n = 5 around 480 Ma). Permian-Carboniferous zircons (n = 5 around 293 Ma) also make an important contribution. Minor zircon populations found are: around 146 Ma (Early Cretaceous, n = 5); around 248 Ma (Triassic, n = 4), around 587 Ma and 621 Ma (Ediacaran, n = 3 each), around 981 Ma (Tonian, n = 4), around 1050 Ma (n = 4, Stenian) and around 1828 Ma (Orosirian, n = 4). The relative probability plot shows a prominent peak around 81 Ma.

On the other hand, sample SP3-91 (Figure 11e), collected higher up in the column, presents most of the zircons between 65-100 Ma (Late Cretaceous), concentrated around 83 Ma (n = 24) and 93 Ma (n = 6) and a mean age for the youngest zircon population of 80 Ma. Other important populations are found around 150 Ma (Jurassic, n = 9), around 296 Ma and around 313 Ma (Permian-Carboniferous, n

= 6 and n = 3, respectively). Other important age peaks were obtained for the Early Cretaceous (102 Ma, n = 3) and the Carboniferous (321 Ma, n = 3). The relative probability has its highest peak around 83 Ma.

Licán Member

The Licán Member (Sample SP3-89; Figure 11f) presents a maximum depositional age of 75 Ma. Its most important populations are in the Permian-Carboniferous range, with n= 23 around 298 Ma, n = 10 around 291 Ma and n = 6 around 309 Ma; it is followed by a 65-100 Ma (Late Cretaceous, n = 19) age peak, with ages grouped around 80 Ma. Minor populations are found around 146 Ma (Early Cretaceous-Late Jurassic, n = 7), 202 Ma and 209 Ma (Triassic, n = 4 and n = 3, respectively). The relative probability plot shows the following age peaks, in decreasing order: 298 Ma, 146 Ma and 80 Ma.

Río Grande Member

The sample obtained from the Río Grande Member (Sample SP3-87; Figure 11g) shows its largest population in the Permian-Carboniferous (n = 51), mainly around 289 Ma. Late Cretaceous zircons (n = 3) are also found, grouped around 73 Ma. The maximum depositional age is 73 Ma. The relative probability plot shows a prominent, distinctive age peak at 289 Ma.

Barros Arana Formation

The Barros Arana Formation (Sample SP3-88; Figure 11h) has a dominant population in the Permian-Carboniferous (n = 25), distributed around 292 Ma. It is followed by other Permian populations around 278 Ma (n = 7) and 265 Ma (n = 3), numerous mid- to Late Cretaceous populations (n = 4 around 78 Ma, n = 4 around 84 Ma, n = 9 around 90 Ma and n = 3 around 97 Ma, for a total of n = 20) and an Early Cretaceous population around 137 Ma (n = 5). The mean age obtained for the youngest population is 78 Ma. The relative probability plot shows age peaks around 292 Ma, 90 Ma and 78 Ma.

In regard to the provenance of the different zircon populations found in these samples, the mid-Cretaceous zircons probably come from the volcanic arc deposits and related intrusives found in the present day Central Valley, such as the Paradero del Desierto Formation (Cortés, 2000) and the Quebrada Mala Formation (Montaño, 1976; Marinovic & García, 1999). Early Cretaceous to Jurassic

zircons were probably derived from the La Negra Arc, which is nowadays exposed in the Coastal Cordillera (Pichowiak *et al.*, 1990; Oliveros *et al.,* 2006). Permian-Triassic ages are found in the Tuina Formation (Figure 2), observed in the area of the same name (Marinovic & Lahsen, 1984; Henríquez *et al.*, in prep.). The El Bordo and Agua Dulce Formations, found to the southwest of the study area, along the El Bordo Escarpment (Ramírez & Gardeweg, 1982; Marinovic & Lahsen, 1984; Basso & Mpodozis, 2012) are also possible sources of Triassic and lower Permian zircons. Other deposits of Permian age have been recorded at the eastern (Cas Formation; Ramírez & Gardeweg, 1982; Breitkreuz, 1995) and southern edges of the Salar de Atacama (Estratos de Cerro Negro; Zimmermann *et al.*, 2009; Niemeyer, 2013).

The important Late Carboniferous to Permian zircon signal seen from the Licán Member upwards is probably related to the lower sections of the mentioned Permian units and the intrusives seen in Cordillera de Domeyko, which are primarily seen in the Precordillera at this latitude, such as the multiple granodioritic intrusions found in the Sierra de Limón Verde (Complejo Intrusivo Limón Verde Indiferenciado; Marinovic & Lahsen, 1984) and the El Bordo and Agua Dulce Formations (Ramírez & Gardeweg, 1982; Breitkreuz *et al.*, 1992; Basso & Mpodozis, 2012). This provenance is consistent with the conglomerate clast counts and paleocurrent data, which is also indicative of an unroofing process of the Precordillera.

Early Carboniferous to Silurian zircons are scarcely found in these samples. Ordovician zircons are abundant in samples K-18 and SP3-90 (La Escalera Member and lower Limón Verde Member, respectively); they are probably derived from the Cordón de Lila Complex (Damm *et al.*, 1990; Zimmermann *et al.*, 2009; Niemeyer, 2013), which would have been at least partially exhumed during the sedimentation of the aforementioned units. Similar ages are also found in the Sierra de Moreno Complex, at Quebrada Chojas, the Belén Metamorphic Complex, Aguada de la Perdiz Formation and in northwestern Argentina; they probably represent equivalents to the Ordovician Ocloyic/Famatinian arc seen in northwestern Argentina (Charrier *et al.*, 2007; Hervé *et al.*, 2007; Sola *et al.*, 2013).

The Cambrian-Neoproterozoic populations seen in samples from the Tonel Formation and lower Limón Verde Member may represent the Pampean arc of which the only close representatives found in Chile are a cordierite-bearing gneiss in the Sierra Limón Verde of 777 ±36 Ma (Damm *et al.*, 1990), and migmatites and schists of the same area (Skarmeta, 1983, *in* Hervé *et al*., 2007); they could

also represent recycled sources. Similar ages are found further to the SE, in Argentina, in the Puncoviscana Formation (Lucassen *et al.*, 2000).

The zircon populations observed between 1000-1200 Ma can be related to the Grenvillian Event (Ramos, 2008, 2010). Rocks with these ages have been found in the Choja Metamorphic Complex (Damm *et al.*, 1990), as part of the Antofalla Basement (Ramos, 2008, 2010). The diamictites of the Sierra Limón Verde also present detrital zircons of this age (Morandé *et al.*, 2012), as well as rocks of the El Toco Formation (Bahlburg *et al.*, 2009), which could indicate some form of recycling. Ages similar to the oldest ones found in the Tonel Formation and Limón Verde Member samples (Figures 11b, 11c and 11d) have only been found far north, in the Belén Metamorphic Complex; they may correspond to the protolith of the Antofalla Basement (Ramos, 2008).

Discussion

The high-resolution stratigraphic columns obtained (Figures 3 and 7) together with the paleocurrents (Figure 8), clast counts (Figure 9), petrographic information (Figure 10) and detrital zircon U-Pb geochronological data (Figure 11) allow the elaboration of an integrated sedimentary and tectonic evolution model of the basin (Figure 12). The Tonel Formation (Figure 12a) presents a fining-upward trend, with the deposition of shallow, gravel- to sand-bed, braided rivers and evaporitic deposits, with an overall NNE-trending flow and andesitic clasts derived from Jurassic-Lower Cretaceous and Permian-Triassic rocks as shown by the detrital zircon data; the maximum depositional ages indicate that this sedimentation could have started around the Jurassic-Cretaceous limit for the lower member (*ca.* 149 Ma), and the mid-Cretaceous (*ca.*107 Ma) for the middle member. The basal to middle Purilactis Formation (Los Cóndores, Limón Verde, Lampallar, Licán and Pajarito Members) begins with mostly shallow, sand- to gravel-bed, braided river deposits, with a W-trending flow (Figure 12b). The detrital zircon populations show the presence of an Upper Cretaceous component, which also sets the maximum depositional age for this part (*ca.*79-75 Ma), and the clasts found are mostly andesites. An important Permian-Carboniferous zircon population becomes evident from the Licán Member onwards, up to the Barros Arana Formation. The Vizcachita Member (Figure 12c) shows paleocurrents opposite to those described before and facies akin to eolian deposits and fluvial intercalations, indicating an arid to semi-arid environment. The upper part of the Purilactis Formation (Figure 12d, e) contains assemblages of shallow, gravel-bed, braided rivers (Seilao Member) and shallow, sand-bed rivers and lacustrine deposits (Río Grande Member). The paleocurrent directions are similar to those of the basal to middle Purilactis Formation, and the maximum depositional ages are also Late Cretaceous (*ca.*73 Ma); the most important population is Permian-Carboniferous in age,

and the clast counts show the progressive increase in crystalline, coarse-grained plutonic fragments compared to andesitic, volcanic fragments, indicating unroofing processes. These clasts become predominant in the Barros Arana Formation, which shows similar detrital zircon patterns, and facies of deep, gravel-bed braided rivers, with a clearer development of cycles and channelization (Figure 12f). Overall, the point-counting data (Figure 10) indicate erosion of a transitional to dissected magmatic arc and an uplifted crystalline basement, though with no clear temporary trend.

This information evidences the increased progradation over time of alluvial fans or proximal braided rivers into the Salar de Atacama Basin and gradual encroaching of the source region, owing to different tectonic pulses. The lack of obvious regional or local unconformities, or progressive deformation, with the exception of those found in the middle member of the Tonel Formation (see above), indicates that the formations were deposited in the (proximal?) foredeep zone of a foreland basin system (DeCelles & Giles, 1996), possibly following mechanisms such as those proposed by Yang & Miall (2010) and Yang (2011). This lack of deformation between members, though more crude, is also seen in seismic sections (Figures 14, 15, Arriagada *et al.*, 2006a).

Many discrepancies have arisen over the years concerning the tectonic setting and precise age of the Mesozoic outcrops in the El Bordo Escarpment. Despite being one of the most studied sectors of the Andes, the lack of robust age data, partly due to the lack of fossils, tuffs or other volcanic units, has led to different models for the basin during the Cretaceous-Paleogene (See above). Most of the 1990's tectonic models regarding the Salar de Atacama Basin were influenced by extensional models, where the Barros Arana Syncline was associated with an inverted graben geometry (Macellari *et al.*, 1991). In this model, the Tonel and Purilactis Formations would have been deposited during the latest Cretaceous-Eocene (Charrier & Reutter, 1990, 1994; Reutter *et al.*, 2006), synchronously with the rift units of the Salta Group in NW Argentina (Salfity *et al.*, 1985; Salfity & Marquillas, 1999; Monaldi *et al.*, 2008). These interpretations, along with those of Hartley *et al.* (1992) and Flint *et al.* (1993) were either based on lithological affinities or the seismic lines obtained by ENAP (Empresa Nacional del Petróleo).

Although the basal part of the Tonel Formation west of the Cerros de Tuina area could have accumulated in the Jurassic-Early Cretaceous, the paleomagnetic data, the ages obtained for the dykes and sills intruding the Tonel and lower Purilactis Formations (Mpodozis *et al*., 2005), and our U-Pb detrital zircon ages account for a mid- to Late Cretaceous age for the middle Tonel and Purilactis Formations. Also, recent regional mapping carried out along the El Bordo Escarpment, south of the study area, has shown that the Barros Arana Syncline can be understood as a footwall growth syncline

developed east of a fault propagation anticline rooted in the Cordillera de Domeyko (Arriagada *et al.*, 2006a). Thus, the western margin of the Salar de Atacama Basin yields evidence for a compressive tectonic setting during, at least, the Late Cretaceous (*ca*. 107 Ma).

Most studies are in agreement concerning the compressive tectonics that occurred during the Paleogene, which are well documented both along the western edge of the basin and within its center (Muñoz *et al.*, 2002; Pananont *et al.*, 2004; Arriagada *et al*., 2006a; Jordan *et al.*, 2007). An important extension event affected this area during the Oligocene, in which the eastern side of the Barros Arana Syncline developed a major normal fault, allowing the accumulation of *ca.* 4000 m of the Oligocene San Pedro Formation, representing most of the current infill (Pananont *et al.*, 2004; Jordan *et al.*, 2007). The recent tectonic history shows clear evidence of compression and active faulting within the modern salar (Jordan *et al*., 2002; Lowenstein *et al.*, 2003; González *et al.*, 2009).

The major differences associated with the various tectonic models proposed can be found in the center of the basin, where all studies are based on the aforementioned seismic lines. Here, the attempts to correlate the outcrops in the El Bordo Escarpment with the units drilled in the Toconao X1 well have been hampered by the high structural style variability observed along the different lines, the poor quality of the seismic lines below 2-3 s TWT and the lack of certainty regarding the presence of deposits belonging to the Purilactis Group in the well. A direct consequence of this is the proliferation of the different, at times contradicting, chronostratigraphic proposals for the basin (Macellari *et al.*, 1991; Flint *et al.*, 1993; Muñoz *et al*., 1997; Muñoz *et al.*, 2002; Pananont *et al*., 2004; Arriagada *et al.*, 2006a; Reutter *et al.*, 2006; Jordan *et al*., 2007). In summary, the Salar de Atacama Basin possesses different, complex events of compressive and extensional deformation, tectonic block rotations and strike-slip deformation imposed over one another, that must be carefully approached in order to fully unravel its internal structure; however, this matter is beyond the scope of this paper.

The U-Pb geochronological data obtained (Figure 11) yield new evidence about the age of the former Purilactis Group. Though the ages obtained for the formations are consistent with the chronostratigraphic chart presented by Mpodozis *et al.* (2005) and Arriagada *et al.* (2006a), several assumptions must be contended; for instance, the accumulation of the lower Purilactis Formation could not take place entirely during the Late Cretaceous normal polarity superchron (119-83.6 Ma), owing to the presence of zircons younger than 85 Ma. The K/Ar ages obtained by Mpodozis *et al*. (2005) in dykes and intrusions in the lower Purilactis and Tonel Formations, together with the data presented here, show that sedimentation of the La Escalera Member might have begun near 107 Ma (Albian) and continued until around 83.6 Ma (Santonian); this coincides with the strong normal

polarity displayed (Arriagada, 1999; Arriagada *et al.*, 2000). The interpretation of the Agua Salada Member data is more complex; though its deposition might have started at 149 Ma, the lack of discordances between members might be more indicative of continuous sedimentation throughout the history of the Tonel Formation since the inception of the foreland basin, or the existence of a paraconformity. No data exist for the Los Cóndores Member, which could have been deposited in the same age range as the La Escalera and Arcoiris Members. Thus, the nature of the time gap between the Tonel and Purilactis Formations cannot be elicited. Sedimentation of the Limón Verde Member could have begun at 79 Ma (Campanian) and continued until no longer than 75 Ma, which is the maximum depositional age obtained for the Licán Member. For the same reasons, the Vizcachita Member cannot represent the magnetic reversal that ended the Late Cretaceous normal polarity superchron (Mpodozis *et al*, 2005); it might record one of the various events that occurred afterwards.

The age limit of the upper Purilactis (Seilao and Río Grande Members) and Barros Arana Formations is not clear; they are bound by the youngest mean zircon age found in the Río Grande Member (see above), which limits its maximum depositional age to the upper Campanian. The only clear geological constraint on the upper limit for the Barros Arana Formation is the presence of the unconformable Oligocene-Miocene Tambores Formation (Flint *et al.,* 1993; Naranjo *et al.*, 1994). A case could be made for their equivalence to the Naranja and/or Loma Amarilla Formations (Mpodozis *et al.*, 2005; Arriagada *et al.*, 2006a), as their northern continuation; however, the age of the youngest population analyzed is older than the ages recorded for both the Cerro Totola and Naranja Formations (Mpodozis *et al*., 2005). Thus, it can be assumed that the Barros Arana Formation might be, at least, older than 58.0±3 Ma (Naranja Formation), and possibly older than the Cerro Totola Formation, as envisioned by Mpodozis *et al.* (2005) and Arriagada *et al.* (2006a).

The provenance information suggests that the Salar de Atacama Basin was receiving sediments from sources even farther to the west than the Cordillera de Domeyko, which also appears to have been uplifted, at least partly, earlier than Eocene-Oligocene times, as previously proposed (Maksaev & Zentilli, 1999); its western border was probably being uplifted during and after the mid-Cretaceous (Figures 13 and 14), while the eastern border, near the southern end of the basin, was subject to tectonism during the K-T and Incaic Events (Arriagada *et al.*, 2006a). The multiple-source provenance is confirmed by the important variations seen in the Tonel Formation and Limón Verde Member samples, which may reflect influx from different tributaries to the system and/or catchment area variations.

The cycles observed in the sedimentary succession and the ages obtained show that the mid-Cretaceous compressive phase was not one event, but rather a long period formed by recurring compressive pulses, similar to the evolution proposed by Noblet *et al.* (1996) for the Central and Northern Andes, particularly for the Quechua and Incaic periods. Interestingly enough, the ages obtained so far are very similar to the ages of the compressive events identified at the Peruvian margin according to Jaillard (1992, 1993). The beginning of sedimentation of the La Escalera Member can be related to the Cenomanian-Albian, Turonian-early Coniacian or late Coniacian-Santonian events; more detailed sampling is required to properly define it. The Limón Verde and Licán Members could be related to the late Campanian event (77-75 Ma), which, according to Jaillard (1992, 1993), is the largest compressive event observed during the Peruvian Phase. Under this scheme, more than 3600 m of sediment accumulated as a result of the latter event, yielding a sedimentation rate of 0.36 mm/Ma for the Purilactis and Barros Arana Formations (not including the Los Cóndores Member). Though deposition of the Barros Arana Formation could have occurred as a product of the K-T event (Cornejo *et al.*, 1997, 2003), the presence of a well-identified K-T unconformity to the west of Calama (Somoza *et al*., 2012), which is not found in the study area, points to the contrary. Also, the ages obtained are older than the fission track ages found around Cerro Quimal, due southwest of the study area, by Andriessen & Reutter (1994), which shows slight uplift of the Cerro Quimal area.

Combining the U-Pb geochronological data with the regional geological information, a model can be proposed where the detrital sources are the product of the exhumation of earlier basins (Figures 13 and 14). The first of these exhumations would have affected parts of the Jurassic-Lower Cretaceous magmatic roots found in the present-day coastal area (Pichowiak *et al.*, 1990; Oliveros *et al.*, 2006), which would explain the Early Cretaceous and Jurassic zircons found in the studied formations (particularly in the Tonel Formation, the Limón Verde and the Licán Members). This event would have also exposed and eroded the Permian-Triassic formations. The next exhumation event would have deformed the mid-Cretaceous deposits of the Central Valley and the successions exposed at the western edge of the Cordillera de Domeyko; this signal is observed from the Limón Verde Member upwards. This exhumation would have also uplifted basement units in the Cordillera de Domeyko area, which is reflected in the abundant Carboniferous-Permian zircons observed from the Licán Member upwards. This process is similar to what has been recorded, though with different timings, in the Chañarcillo and Lautaro Basins due south in the Atacama Region (27°-28°S), over the flat-slab region (Martínez *et al.*, 2012, 2013).

These two steps effectively separate the Peruvian or mid-Cretaceous compressional phase into two different stages; the "early" Peruvian Phase (probably the same as the "Mochica" phase proposed by Mégard, 1984) involved strong compression and uplift of the present Coastal Cordillera area and had minor effects on other sectors close to the actual Salar de Atacama area, between 107 Ma and 83.6 Ma. This is reflected in the facies belonging to the mid- to upper-Tonel Formation, which are less thick and finer-grained than the Purilactis and Barros Arana Formations, probably reflecting a more distal deposition. On the other hand, the "late" Peruvian Phase shows an eastward jump of the main deformation area, strongly involving the mid-Cretaceous arc units (see above) and the Cordillera de Domeyko area, reflected in the deposition of the Purilactis and Barros Arana Formations, from 79 Ma to 65 Ma. Sedimentation of the Barros Arana Formation is ended by the K-T Event, shown by the deposition of the Cerro Totola Formation, the Naranja Formation, and then the Loma Amarilla Formation during the Incaic Event during the Late Eocene-Early Oligocene (Arriagada, 1999; Mpodozis *et al.,* 2005; Arriagada *et al.,* 2006a).

It can be seen then that the Salar de Atacama Basin does not behave like a classic foreland basin system *sensu* DeCelles & Giles (1996); instead of progressing continuously to the east, the orogenic wedge appears to have been broken several times during the Late Cretaceous. Though one could still consider all basement blocks west of the basin as part of the orogenic front, its internal structure is far more complicated. The Tolar and Tambillo Basins (Tomlinson *et al.,* 2001), found to the northwest of the study area, could be considered as intra-montane (piggy-back?) basins, and part of the system as a whole.

More evidence for early uplift in this sector during mid-Cretaceous times has been found as far east as the Puna of NW Argentina, where apatite fission track (AFT) dating performed on the Eocene Geste Formation found AFT cooling ages between 88-112 Ma, which are explained as a distant signal coming from the Cordillera de Domeyko area (Carrapa & DeCelles, 2008). It is possible then that some formations interpreted to have been deposited in extensional basins, could in fact be compressive in nature; in the case of the Quebrada Mala Formation, the kinematics of the Sierra del Buitre Fault, which controls the deposition of the formation (Marinovic & García, 1999) are not distinctively clear. Andriessen & Reutter (1994) also pointed to the intrusion of the 80 Ma San Cristóbal Pluton in folded Jurassic-Lower Cretaceous deposits as evidence of deformation in the Santonian. They also showed concordant fission track ages of 72 Ma obtained from granitic stocks in Sierra de Navidad, which may indicate a tectonic event around that age; however, the results were not conclusive. In the case of the Cerrillos Formation, interpreted by Martínez *et al*. (2013) as a post-rift succession, Maksaev *et al*. (2009) concluded that its coarse conglomeratic facies provide evidence of

tectonic uplift during the middle to late Aptian. Close to this area, around 28º30'S, Merino *et al.* (2013) suggested tectonic unroofing of Lower Cretaceous units in the Coastal Cordillera between 90-85 Ma, reflected in the deposition of the Quebrada Seca Formation. It is interesting to note that the Tonel Formation is a time-equivalent of the Quebrada Seca and Cerrillos Formations, while the Hornitos Formation (Martínez *et al.*, 2013) seems to be related to the Purilactis and Barros Arana Formations. Similar ages for the beginning of compression have been obtained for the Coastal Range of Central Chile, in the Caleu Pluton and the Las Chilcas Formation (Parada *et al*., 2005); thus, a broader picture can be conceived where the entire western margin was undergoing compression from mid-Cretaceous times onward.

Conclusions

The Tonel, Purilactis and Barros Arana Formations show a diverse range of facies, accounting for more than 4000 m of sedimentation since the mid-Cretaceous, during the entire Peruvian Phase. The Tonel Formation shows shallow, gravel-bed, braided river facies (Agua Salada Member), which gradually change upward into fine-grained facies representing a transition to a more distal, possibly lacustrine or overbank environment (La Escalera and Arcoiris Members). The Los Cóndores Member shows sheetflood sandstones belonging to distal braid-plains and sand-bed rivers. The Limón Verde Member presents distal, braided, sand-dominated river deposits, or ephemeral sheetflood sediments in mostly arid regions with shallow channel depths, with an upward manifestation of deeper, gravel-bed, braided river deposits. The Lampallar, Licán and Pajarito Members show laminated sandstones, related to slightly channelized, ephemeral, sand-bed rivers, and mostly clast-supported, stratified conglomerates probably deposited in shallow, gravel-bed braided rivers with scarce gravity flow deposits. It grades into the Vizcachita Member, dominated by eolian deposits. The Seilao Member shows a return to coarse facies, interpreted as shallow, gravel-bed braided rivers, with intervals dominated by ephemeral sheetflood deposits which grade into the Río Grande Member, showing an abundance of lithofacies related to ephemeral, poorly confined sand-bed rivers and lacustrine deposits. Finally, the Barros Arana Formation exhibits facies typical of deep, gravel-bed braided rivers and flashflood deposits. Provenance data, conglomerate clast counts and the U-Pb detrital zircon geochronology show that the source of sediments was extremely diverse, reflecting the entire uplift of the arc and back-arc deposits. Sediment transport followed mainly a northeast-eastward direction. The age of these deposits ranges from 149 Ma (Tithonian) to 107 Ma (Albian) for the Agua Salada Member, 107 Ma to 83.6 Ma (Santonian) for the La Escalera Member, the Arcoiris Member and, possibly, the Los Cóndores Member, and 79 Ma (Campanian) to 65 Ma (Paleocene) for the rest of the Purilactis and Barros Arana Formations.

The facies variations are intimately associated with the development of the Peruvian Phase; the "early" Peruvian Phase (around 107-83.6 Ma) encompassed deposition of the La Escalera Member, the Arcoiris and the Los Cóndores Members, while the "later" Peruvian Phase (79-65 Ma) witnessed deposition of most of the Purilactis and Barros Arana Formations. While the former event shows deformation and uplift of the Cordillera de la Costa area, the latter presents an eastward jump of the orogenic front to the present Cordillera de Domeyko area. The units were most likely deposited in a foredeep setting, with an increasing proximity to the orogenic front; the front itself is partly a result of the exhumation and cannibalization of previous basins. The different events clearly broke the orogenic wedge into different sections, allowing the appearance of different sources reflected in the stratigraphic record.

In a regional context, these results are in accordance with the age of compression seen elsewhere in north-central Chile and the western margin of South America, and provide new information for the Mesozoic to Cenozoic evolution of the northern Central Andes.

Table 1. Simplified chronostratigraphic chart.

Table 2. Lithofacies code

Table 3. Parameters for sandstone point counting.

Figure 1: a) Map of the western margin of South America, showing its mainstructures. From west to east; light blue: Coastal Cordillera; pink: Longitudinal Valley; grey: Precordillera; red: Salar de Atacama Basin; purple: Western Cordillera; blue: Altiplano-Puna; brown: Eastern Cordillera; yellow: Sub Andean Ranges; green: Santa Barbara and the Sierras Pampeanas. b) Main tectonic features of the Andes between 22° and 24°S. The study area is inside the white rectangle.

Figure 2: Geological map of the study area, showing the location of the U/Pb samples and the columns profiled. Modified from Henríquez *et al.* (in prep.).

Figure 3: a) Measured and b) compiled stratigraphic column of the Tonel, Purilactis and Barros Arana Formation. Stippled lines indicate parts of the measured column used for the compilation. Tendency line equation shown at the top right corner of a), showing an overall increase in grain size. Covered areas were estimated with Google Earth. Los Cóndores Member compiled from previous studies (see text). The Arcoiris Member was not measured.

Figure 4: Facies and outcrops observed in the area: a) Planar cross-stratified conglomerates (Gpt). b) Imbricated horizontally stratified conglomerates (Gch). c) Burrows in laminated sandstones (Sh). d) Massive, clast-supported conglomerates (Gcm) showing erosional contacts with medium-grained sandstones (Sl). e) Trough cross-stratified sandstones. f) Horizontally stratified, clast-supported conglomerates (Gch) intercalated with medium- to coarse-grained sandstones (Sl).

Figure 5: a) Laminated, fine- to medium-grained sandstones (Sh) of the Tonel Formation (La Escalera Member). b) Sandstones and conglomerates of the Limón Verde Member. c) Laminated, fine- to medium-grained sandstones (Sh) interbedded with clast-supported, horizontally stratified conglomerates (Gch), seen in the Lampallar Member. d) Similar deposits of the Licán Member. e) Paleodunes in the Vizcachita Member. f) Typical clast-supported, horizontally laminated conglomerates (Gch) of the Seilao Member. g) Burrows between laminated sandstones and conglomerates of the Barros Arana Formation.

Figure 6: a) Sandstones of the Purilactis Formation (Limón Verde and Los Cóndores Members) overlying sandstones and deformed evaporitic deposits of the Tonel Formation (Arcoiris Member), at the southern end of the Barros Arana Syncline. b) Closer picture of the aforementioned contact. c) Gradational contact between the Vizachita and Pajarito Members.

Figure 7: High-resolution stratigraphic sections of the studied members and formations.

Figure 8: Paleocurrent directions obtained in this study. Directions plotted with GeoRose 0.3.0 software developed by Yong Technology Inc. The Licán Member includes measurements of the Pajarito and Lampallar Members.

Figure 9: Conglomerate clast-count of the units investigated in this study. 100 clasts were counted in each station. The counts marked with an asterisk are qualitative.

Figure 10: Sandstone petrographic data: a) Qm-F-Lt and b) Qt-F-L diagrams. Fields after Dickinson et al. (1983). 1: Craton Interior. 2: Transitional Continental. 3: Basement Uplift. 4: Quartzose Recycled. 5: Mixed. 6: Dissected Arc. 7: Transitional Arc. 8: Undissected Arc. 9: Lithic Recycled. 10: Transitional Recycled. c) Qp-Lv-Ls, d) Qt-F-L, e) Qm-F-Lt and f) Qm-P-K after Weltje (2006). A: Continental Block Provenance. B: Magmatic Arc Provenance. C: Recycled Orogen Provenance. g) Qp-Lv-Fp, after Ingersoll (2012). U: Undissected Arc. T: Transitional Arc. R: Recycled Orogen. B: Basement Uplift.

Figure 11: U/Pb detrital zircon ages for the Tonel (a, b and c), Purilactis (d, e, f and g) and Barros Arana (h) Formations. Sample locations in Figure 2.

Figure 12: Facies evolution of the Salar de Atacama Basin during the mid-Cretaceous to Paleogene. a) Basal gravel- to mostly sand-braided river and lacustrine deposits of the Tonel Formation and part of the Los Cóndores Member. b) Mainly sand-braided rivers and distal alluvial fans of the Limón Verde, Lampallar, Licán and Pajarito Members. c) Eolian dunes representing the Vizcachita Member. d) Shallow, gravel-braided rivers and alluvial fans of the Seilao Member. e) Fluvial and lacustrine deposits of the Río Grande Member. f) Deep, gravel-braided rivers and alluvial fans of the Barros Arana Formation. Blue arrows indicate major paleocurrent directions. The Tuina area (in pink) has been rotated 30° counterclockwise. Light grey area indicates the present-day western Cordillera de Domeyko outcrop limit. Light-stippled line shows the hypothetical foredeep section of the basin. Crosses indicate positive relief.

Figure 13: Basin exhumation and compression in northern Chile. Modified from Servicio Nacional de Geología y Mineria (2003).

Figure 14: Schematic cross-section of northern Chile between 22°-23°S, showing basin and orogenic wedge evolution. The figure also shows a hypothetical, eroded forearc.

Supporting Information

Appendix A. Detailed stratigraphic sections profiled in this study.

Appendix B. Provenance (point-counting) raw data.

Appendix C. Detrital zircon data.

Acknowledgements

The authors would like to thank and acknowledge the contributions and funding by the SERNAGEOMIN 1:100.000 National Mapping Project. Sergio Villagrán, Marco Vaccaris, Katherine Narea, Iván Gómez, Susana Henríquez, Juan Becerra and the Laboratorio de Tectónica y Paleomagnetismo of the Universidad de Chile are thanked for their field support and work. The authors declare that they have read the "Conflict of Interest" statement by Basin Research, and that they have no conflict of interest to report. We are grateful to Basin Research Editor Sébastien Castelltort, Andrés Folguera, Alberto Resentini and Peter DeCelles for their suggestions on how to improve the manuscript.

References

ALLMENDINGER, R.W., JORDAN, T.E., KAY, S.M. & ISACKS, B.I. (1997) The evolution of the Altiplano-Puna Plateau of the Central Andes. *Annual Reviews Earth Planetary Science Letters*, 25, 139-174.

AMILIBIA, A., SÁBAT, F., MCCLAY, K.R., MUÑOZ, J.A., ROCA, E. & CHONG, G. (2008) The role of inherited tectono-sedimentary architecture in the development of the central Andean mountain belt: Insights from the Cordillera de Domeyko. *Journal of Structural Geology*, 30 (12), 1520-1539.

ANDRIESSEN, P.A.M. & REUTTER, K.J. (1994) K-Ar and fission track mineral age determination of igneous rocks related to multiple magmatic arc systems along the 23°S latitude of Chile and NW Argentina. In *Tectonics of the Southern Central Andes: Structure and Evolution of an Active Continental Margin* (Ed. by K.J. Reutter, E. Scheuber, and P. Wigger), pp. 141-154. Springer, New York.

ARRIAGADA, C. (1999) Geología y Paleomagnetismo del Borde Oriental de la Cordillera de Domeyko entre los 22°45' y 23°30' latitud Sur. II Región, Chile. *MSc. Thesis, Universidad de Chile*, (unpublished), p.176.

ARRIAGADA, C., ROPERCH, P. & MPODOZIS, C. (2000) Clockwise block rotations along the eastern border of the Cordillera de Domeyko, northern Chile (22°45'–23°30'S). *Tectonophysics*, 326, 153 – 171.

ARRIAGADA, C., ROPERCH, P., MPODOZIS, C., DUPONT-NIVET, G., COBBOLD. P.R., CHAUVIN, A. & CORTÉS, J. (2003) Paleogene clockwise tectonic rotations in the forearc of central Andes, Antofagasta region, northern Chile. *Journal of Geophysical Research*,18, B1 2032. doi:10.1029/2001JB001598

ARRIAGADA, C., COBBOLD, P.R. & ROPERCH, P. (2006a) The Salar de Atacama basin: a record of Cretaceous to Paleogene compressional tectonics in the Central Andes. *Tectonics*, 25, TC1008, doi:10.1029/2004TC001770.

ARRIAGADA, C., ROPERCH, P., MPODOZIS, C. & FERNANDEZ, R. (2006b) Paleomagnetism and tectonics of the southern Atacama Desert (25-28°S), northern Chile. *Tectonics*, 25, TC4001, doi: 10.1029/2005TC001923.

ARRIAGADA, C., ROPERCH, P., MPODOZIS, C. & COBBOLD, P.R. (2008) Paleogene building of the Bolivian Orocline: Tectonic restoration of the central Andes in 2-D map view. *Tectonics*, 27, TC6014, doi: 10.1029/2008TC002269.

BAHLBURG, H., VERVOORT, J.D., DU FRANE, S.A., BOCK, B., AUGUSTSSON, C. & REIMANN, C. (2009) Timing of crust formation and recycling in accretionary orogens: Insights learned from the western margin of South America. *Earth-Science Reviews*, 97, 215-241.

BASSO, M. & MPODOZIS, C. (2012) Carta Cerro Quimal, Región de Antofagasta. Servicio Nacional de Geología y Minería, Carta Geológica de Chile, *Serie Geología Básica*, 143, 1-46. 1 mapa escala 1:100.000. Santiago, Chile.

BREITKREUZ, C., HELMDACH, F.F., KOHRING, R. & MOSBRUGGER, V. (1992) Late Carboniferous Intra-arc sediments in the north Chilean Andes: Stratrigraphy, Paleogeograhpy and Paleoclimate. *Facies*, 26, 67-80.

BREITKREUZ, C. (1995) The Late Permian Peine and Cas Formations at the eastern margin of the Salar de Atacama, Northern Chile: stratigraphy, volcanic facies, and tectonics. *Revista Geológica de Chile*, 22, 3-23.

BREITKREUZ, C. & VAN SCHMUS, W.R. (1996) U–Pb geochronology and significance of Late Permian ignimbrites in Northern Chile. *Journal of South American Earth Sciences*, 9 (5/6), 281– 293.

BRÜGGEN, J. (1934) Las Formaciones de Sal y Petróleo de la Puna de Atacama. *Boletín de Minas y Petróleo*, 32, 105-122. Santiago, Chile.

BRÜGGEN, J. (1942) Geología de la Puna de San Pedro de Atacama y sus formaciones areniscas y arcillas rojas. In *Congreso Panamericano de Ingeniería de Minas y Geológica, Actas*, 2, 342-467. Santiago, Chile.

BRÜGGEN, J. (1950) Fundamentos de la Geología de Chile. *Instituto Geográfico Militar*: 1 – 374. Santiago, Chile.

CARRAPA, B. & DECELLES, P.G. (2008) Eocene exhumation and basin development in the Puna of northwestern Argentina. *Tectonics*, 27, TC1015, doi: 10.1029/2007TC002127.

CARRAPA, B., BYWATER-REYES, S., DECELLES, P.G., MORTIMER, E. & GEHRELS, G.E. (2012) Late Eocene–Pliocene basin evolution in the Eastern Cordillera of northwestern Argentina (25°–26°S): regional implications for Andean orogenic wedge development. *Basin Research*, 24, 249–268. doi: 10.1111/j.1365-2117.2011.00519.x

CHARRIER, R. & REUTTER, K.J. (1990) The Purilactis group of Northern Chile: link between arc and backarc during Late Cretaceous and Paleogene. In *Proceedings I ORSTOM-ISAG*: 249–252. Grenoble, France.

CHARRIER, R. & MUÑOZ, N. (1994) Jurassic-Cretaceous Paleogeographic evolution of the Chilean Andes at 23°-24°S.L. and 34°-35°S.L.: a comparative analysis. In *Tectonics of the Southern Central Andes: Structure and Evolution of an Active Continental Margin* (Ed. by K.J. Reutter, E. Scheuber and P. Wigger), pp. 233-242. Springer, New York.

CHARRIER, R. & REUTTER, K.J. (1994) The Purilactis group of northern Chile: Boundary between arc and backarc from Late Cretaceous to Eocene. In *Tectonics of the Southern Central Andes: Structure and Evolution of an Active Continental Margin* (Ed. by K.J. Reutter, E. Scheuber and P. Wigger), pp. 189-202. Springer, New York.

CHARRIER, R., PINTO, L. & RODRÍGUEZ, M.P. (2007) Tectonostratigraphic evolution of the Andean Orogen in Chile. In *The Geology of Chile* (Ed. by T. Moreno and W. Gibbons), pp. 21-114. The Geological Society, London.

CHARRIER, R., FARÍAS, M. & MAKSAEV, V. (2009) Evolución tectónica, paleogeográfica y metalogénica durante el Cenozoico en los Andes de Chile norte y central e implicaciones para las regiones adyacentes de Bolivia y Argentina. *Revista de la Asociación Geológica Argentina*, 65 (1), 5-35.

COBBOLD, P.R. & ROSELLO, E.A. (2003) Aptian to recent compressional deformation, foothills of the Neuquén Basin, Argentina. *Marine and Petroleum Geology*, 20, 429-443.

COBBOLD, P.R., ROSELLO, E.A. ROPERCH, P., ARRIAGADA, C., GÓMEZ, L.A. & LIMA, C. (2007) Distribution and timing of Andean deformation across South America. In *Global Tectonic Processes: The legacy of Mike Coward* (Ed. by A. Ries, R.H. Graham and R.W. Butler). Geological Society Special Publications..

COIRA, B., KOUKHARSKY, M., RIBEIRO GUEVARA, S. & CISTERNA, C.E. (2009) Puna (Argentina) and northern Chile Ordovician Basic Magmatism: A contribution to the tectonic setting. *Journal of South American Earth Sciences*, 27, 24-35.

CORNEJO, P., TOSDAL, R.M., MPODOZIS, C., TOMLINSON, A.J., RIVERA, O. & FANNING, M. (1997) El Salvador, Chile porphyry copper deposit revisited: geologic and geochronologic framework. *International Geology Review*, 39, 22-54

CORNEJO, P., MATTHEWS, S. & PÉREZ, C. (2003) The "K-T" compressive deformation event in northern Chile (24°-27°S). In *Proceedings 10th Congreso Geológico Chileno*. Concepción, Chile.

CORTÉS, J. (2000) Hoja Palestina, Región de Antofagasta. Servicio Nacional de Geología y Minería, *Mapas Geológicos*, 19. 1 mapa escala 1:100.000. Santiago, Chile.

DAMM, K.W., PICHOWIAK, S., HARMON, R.S., TODT, W., KELLEY, R., OMARINI, R. & NIEMEYER, H. (1990) Pre-Mesozoic evolution of the central Andes: The basement revisited. *Geological Society of America Special Papers*, 241, 101-126.

DECELLES, P.G., LANGFORD, R.P. & SCHWARTZ, R.K. (1983) Two new methods of paleocurrent determination from trough cross-stratification. *Journal of Sedimentary Petrology*, 53, 629-642.

DECELLES, P.G. & GILLES, K.A. (1996) Foreland basin systems. *Basin Research*, 8, 105-123.

DECELLES, P.G., CARRAPA, B., HORTON, B.K. & GEHRELS, G.E. (2011) Cenozoic foreland basin system in the central Andes of northwestern Argentina: Implications for Andean geodynamics and modes of deformation. *Tectonics*, 30, TC6013. 2011 doi:10.1029/2011TC002948

DICKINSON, W.R.(1970) Interpreting detrital modes of greywacke and arkose. *Journal of Sedimentary Petrology*, 40, 695-707.

DICKINSON, W.R. & SUCZEK, C.A. (1979) Plate tectonics and sandstone composition. *American Association of Petroleum Geologists Bulletin*, 63, 2164-2182.

DICKINSON, W.R., BEARD, L.S., BRAKENRIDGE, G.R., ERJAVEC, J.L., FERGUSON, R.C., INMAN, K.F., KNEPP, R.A., LINDBERG, A. & RYBERG, P.T. (1983) Provenance of North American Phanerozoic sandstones in relation to tectonic. *Geological Society of America Bulletin*, 94, 222-235.

DICKINSON, W.R. (1985) Interpreting provenance relation from detrital modes of sandstones. In *Provenance of Arenites* (Ed. by G.G Zuffa), pp. 333-363. D. Reidel, Dordrecht, Netherlands.

DINGMAN, R.J. (1963) Cuadrángulo Tulor. Instituto de Investigaciones Geológicas, *Carta Geológica de Chile*, 11, 1-35. 1 mapa escala 1:50.000. Santiago, Chile.

DINGMAN, R.J. (1967) Geology and Groundwater Resources of the Northern part of the Salar de Atacama, Antofagasta Province, Chile. *U.S. Geological Survey Bulletin*, 1219, 1-49.

FLINT, S., HARTLEY, A., REX, D., GUISE, P. & TURNER, P. (1989) Geochronology of the Purilactis Formation, Northern Chile: an insight into Late Cretaceous/Early Tertiary basin dynamics of the Central Andes. *Revista Geológica de Chile*, 16, 241–246.

FLINT, S., TURNER, P., JOLLEY, E.J. & HARTLEY, A.J. (1993) Extensional tectonics in convergent margin basins: An example from the Salar de Atacama, Chilean Andes. *Geological Society of America Bulletin*, 105, 603-617.

GONZÁLEZ, G., CEMBRANO, J., ARON, F., VELOSO, E.E. & SHYU, J.B.H. (2009) Coeval compressional deformation and volcanism in the central Andes, case studies from northern Chile (23°S-24°S). *Tectonics*, 28, TC6003, doi: 10.1029/2009TC002538.

GÖTZE, H.J. & KRAUSE, S. (2002) The central Andean gravity high, a relic of an old subduction complex?. *Journal of South American Earth Sciences*, 14, 799-811.

HAMMERSCHMIDT, K., DÖBEL, R. & FRIEDRICHSEN, H. (1992) Implication of $^{40}Ar/^{39}Ar$ dating of Early Tertiary volcanic rocks from the north-Chilean Precordillera. *Tectonophysics*, 202, 55-81.

HARTLEY, A., FLINT, S. & TURNER, P. (1988) A proposed lithostratigraphy for the Cretaceous Purilactis Formation, Antofagasta Province, northern Chile. In *Congreso Geológico Chileno No. 5 Actas*, 3, H83–H99. Santiago.

HARTLEY, A.J., FLINT, S., TURNER, P. & JOLLEY, E.J. (1992) Tectonic controls on the development of a semiarid, alluvial basin as reflected in the stratigraphy of the Purilactis Group (upper Cretaceous-Eocene), northern Chile. *Journal of South American Earth Sciences*, 5, 275-296.

HARTLEY, A.J. (1993) Sedimentological response of an alluvial system to source area tectonism: the Seilao Member of the Late Cretaceous to Eocene Purilactis Formation of northern Chile. In *Alluvial Sedimentation: International Association of Sedimentologists Special Publication 17* (Ed. by M. Marzo and C. Puigdefabregas), pp. 489-500. Blackwell Publishing Ltd., Oxford, London.

HARVEY, A.M. (1984) Debris flows and fluvial deposits in Spanish Quaternary alluvial fans: implications for fan morphology. In *Sedimentology of Gravels and Conglomerates, Memoir 10* (Ed. by E.H. Koster and R.J. Steel), pp. 123-132. Canadian Society of Petroleum Geologists, Calgary, Alberta, Canada.

HEIN, F.J. (1984) Deep-sea and fluvial braided channel conglomerates: A comparison of two case studies. In *Sedimentology of Gravels and Conglomerates, Memoir 10* (Ed. by E.H. Koster and R.J. Steel), pp. 33-49. Canadian Society of Petroleum Geologists, Calgary, Alberta, Canada.

HENRÍQUEZ, S.M., BECERRA, J. & ARRIAGADA, C. (In prep.) Geología del área San Pedro de Atacama, Región de Antofagasta. Servicio Nacional de Geología y Mineria. *Carta Geológica de Chile, Serie Geología Básica*. 1 mapa escala 1:100.000. Santiago, Chile.

HERVÉ, F., FAUNDEZ, V., CALDERÓN, M., MASSONE, H.J. & WILLNER, A.P. (2007) Metamorphic and plutonic basement complexes. In *The Geology of Chile* (Ed. by T. Moreno and W. Gibbons), pp. 5-20. The Geological Society, London.

INGERSOLL, R.V., BULLARD, T.F., FORD, R.L., GRIMM, J.P., PICKLE, J.D. & SARES, S.W. (1984) The effect of grain size on detrital modes: A test of the Gazzi-Dickinson point-counting method. *Journal of Sedimentary Research*, 54, 103-116.

INGERSOLL, R.V. (2012) Composition of modern sand and Cretaceous sandstone derived from the Sierra Nevada, California, USA, with implications for Cenozoic and Mesozoic uplift and dissection. *Sedimentary Geology*, 280, 195-207.

ISACKS, B.L. (1988) Uplift of the central Andean plateau and bending of the Bolivian orocline. *Journal of Geophysical Research*, 93, 3211 – 3231.

JAILLARD, E. (1992) La Fase Peruana (Cretáceo Superior) en la Margen Peruana. *Boletín de la Sociedad Geológica del Perú*, 83, 81-87.

JAILLARD, E. (1993) L'évolution tectonique de la marge péruvienne au Sénonien et Paléocene et ses relations avec la geodynamique. *Bulletin de la Société Géologique de France*, 164, n°6, 819-830.

JAILLARD, E.; BENGTSON, P. & DHONDT, A.V. (2005) Late Cretaceous marine transgressions in Ecuador and northern Peru: a refined stratigraphic framework. *Journal of South American Earth Sciences*, 19, 307-323.

JAIMES, E. & DE FREITAS, M. (2006) An Albian-Cenomanian unconformity in the northern Andes: evidence and tectonic significance. *Journal of South American Earth Sciences*, 21, 466-492.

JOLLEY, E.J., TURNER, P., WILLIAMS, G.D., HARTLEY, A.J. & FLINT, S. (1990) Sedimentological response of an alluvial system to Neogene thrust tectonics, Atacama Desert, northern Chile. *Journal of the Geological Society, London*, 147, 769-784.

JORDAN, T.E., MUÑOZ, N., HEIN, M., LOWENSTEIN, T., GODFREY, L. & YU, J. (2002) Active faulting and folding without topographic expression in an evaporite basin, Chile. *Geological Society of America Bulletin*, 114, 1406-1421.

JORDAN, T.E., MPODOZIS, C., MUÑOZ, N., BLANCO, N., PANANONT, P. & GARDEWEG, M. (2007) Cenozoic subsurface stratigraphy and structure of the Salar de Atacama Basin, northern Chile. *Journal of South American Earth Sciences*, 23, 122-146.

KOCUREK, G. (1981) Significance of interdune deposits and bounding surfaces in aeolian dune sands. *Sedimentology*, 28, 753-780.

KOCUREK, G. (1991) Interpretation of ancient eolian sand dunes. *Annual Reviews Earth Planetary Science Letters*, 19, 43-75.

LE ROUX, J.P. (1991) Paleocurrent analysis using Lotus 1-2-3. *Computers & Geosciences* , 17, no. 10,1465-1468.

LE ROUX, J.P. (2012) A review of Tertiary climate changes in southern South America and the Antarctic Peninsula. Part 2: continental conditions. *Sedimentary Geology*, 247-248, 21-38.

LOWENSTEIN, T.K., HEIN, M.C., BOBST, A.L., JORDAN, T.E., KU, T. & LUO, S. (2003) An assessment of stratigraphic completeness in climate-sensitive closed-basin lake sediments: Salar de Atacama, Chile. *Journal of Sedimentary Research*, 73, 91-104.

LUCASSEN, F., BECCHIO, R., WILKE, H.G., FRANZ, G., THIRLWALL, M.F., VIRAMONTE, J. & WEMMER, K. (2000) Proterozoic-Paleozoic development of the basement of the Central Andes (18-26°S) – a mobile belt of the South American craton. *Journal of South American Earth Sciences*, 13, 697-715.

LUDWIG, K.R. (2008) Isoplot 3.6. *Berkeley Geochronology Center Special Publication*, 4, 1-77.

MACELLARI, C.E., SU, M.J. & TOWNSEND, F. (1991) Structure and seismic stratigraphy of the Atacama Basin (northern Chile). In *Congreso Geológico Chileno No. 6 Actas*, 1, 133-137. Viña del Mar, Chile.

MAKSAEV, V. & ZENTILLI, M. (1999) Fission track thermochronology of the Domeyko Cordillera, northern Chile: Implications for Andean tectonics and porphyry copper metallogenesis. *Exploration and Mining Geology*, 8, 65-89.

MAKSAEV, V., MUNIZAGA, F., VALENCIA, V. & BARRA, F. (2009) LA-ICP-MS zircon U-Pb geochronology to constrain the age of post-Neocomian continental deposits of the Cerrillos Formation, Atacama Region, northern Chile: tectonic and metallogenic implications. *Andean Geology*, 36 (2), 264-287.

MARINOVIC, N. & LAHSEN, A. (1984) Hoja Calama. Servicio Nacional de Geología y Minería, *Carta Geológica de Chile*, 58, 1-140. 1 mapa escala 1:250.000. Santiago, Chile.

MARINOVIC, N. & GARCÍA, M. (1999) Hoja Pampa Unión. Región de Antofagasta. Servicio Nacional de Geología y Minería, *Mapas Geológicos*, 9. 1 mapa escala 1:100.000. Santiago, Chile.

MARTINEZ, F., ARRIAGADA, C., MPODOZIS, C. & PEÑA, M. (2012) The Lautaro Basin: a record of inversión tectonics in nothern Chile. *Andean Geology*, 39 (2), 258-278.

MARTÍNEZ, F., ARRIAGADA, C., PEÑA, M., DEL REAL, I. & DECKART, K. (2013) The structure of the Chañarcillo Basin: An example of tectonic inversión in the Atacama region, northern Chile. *Journal of South American Earth Sciences*, 42, 1-16.

MÉGARD, F. (1984) The Andean orogenic period and its major structures in central and northern Peru. *Journal of the Geological Society of London*, 141, 893-900.

MERINO, R., SALAZAR, E., MORA-FRANCO, C., CREIXELL, C., COLOMA, F. & OLIVEROS, V. (2013) Fluvial deposition and retro-arc volcanism in a Late Cretaceous foreland basin and the unroofing of the Early Cretaceous arc in the chilean Frontal Cordillera at 28º30'S, Atacama Region. *Bolletino di Geofisica: teorica ed applicata*, Vol.54, Supplement 2, 237-238.

MIALL, A.D. (1985) Architectural element analysis: A new method of facies analysis applied to fluvial deposits. *Earth Science Reviews*, 22, 261-308.

MIALL, A.D. (1996). *The Geology of Fluvial Deposits. Sedimentary Facies, Basin Analysis and Petroleum Geology*. Springer-Verlag, New York.

MONALDI, C.R., SALFITY, J.A. & KLEY, J. (2008) Preserved extensional structures in an inverted Cretaceous rift basin, northwestern Argentina: Outcrop examples and implications for fault reactivation. *Tectonics*, 27, TC1011, doi: 10.1029/2006TC001993.

MONTAÑO, J.M. (1976) Estudio geológico de la zona de Caracoles y áreas vecinas, con énfasis en el Sistema Jurásico, Provincia de Antofagasta, II Región, Chile. *Bsc. Thesis, Universidad de Chile*, (unpublished), p.168.

MORANDÉ, J., MPODOZIS, C., VALENCIA, V., ARRIAGADA, C. & MARQUARDT, C. (2012) Las Diamictitas de Sierra Limón Verde, Antofagasta: Evidencias de Glaciación Neoproterozoica en el Norte de Chile?. In *Congreso Geológico Chileno XIII Actas*, T2, 271-273. Antofagasta, Chile.

MPODOZIS, C., ARRIAGADA, C. & ROPERCH, P. (1999) Cretaceous to Paleogene geology of the Salar de Atacama basin, northern Chile: A reappraisal of the Purilactis Group stratigraphy. In *Proceedings IV IRD-ISAG*, 523-526. Göttingen.

MPODOZIS, C., ARRIAGADA, C., BASSO, M., ROPERCH, P., COBBOLD, P. & REICH, M. (2005) Late Mesozoic to Paleogene stratigraphy of the Salar de Atacama basin, Antofagasta, northern Chile: Implications for the tectonic evolution of the central Andes. *Tectonophysics*, 399, 125-154.

MUÑOZ, N., CHARRIER, R. & REUTTER, K. (1997) Evolución de la cuenca Salar de Atacama: Inversión tectónica y relleno de una cuenca de antepaís de retroarco. In *Congreso Geológico Chileno No. 8 Actas*, 1, 195-199. Antofagasta.

MUÑOZ, N., JORDAN, T.E. & CHARRIER, R. (2002) Interactions between basement and cover during the evolution of the Salar de Atacama basin, northern Chile. *Revista Geológica de Chile*, 29, 3-29.

NALPAS, T., DABARD, M.P., RUFFET, G., VERNON, A., MPODOZIS, C., LOI, A. & HÉRAIL, G. (2008) Sedimentation and preservation of the Miocene Atacama Gravels in the Pedernales Chañaral area, Northern Chile: climatic or tectonic control?. *Tectonophysics*, 459, 161–173.

NARANJO, J.A., RAMÍREZ, C.F. & PASKOFF, R. (1994) Morphostratigraphic evolution of the northwestern margin of the Salar de Atacama basin (23°S-68°W). *Revista Geológica de Chile*, 21, 91-103.

NEMEC, W. & STEEL, R.J. (1984) Alluvial and coastal conglomerates: their significant features and some comments on gravelly mass-flow deposits. In *Sedimentology of Gravels and Conglomerates* (Ed. by E.H. Koster and R.J. Steel, R.J.), *Canadian Society of Petroleum Geologists Memoir*, 10, 1-31.

NIEMEYER, R.H. (1989) El Complejo Ígneo-Sedimentario del Cordón de Lila, Región de Antofagasta: significado tectónico. *Revista Geológica de Chile*, 16(2), 163-181.

NIEMEYER, H. (2013) Geología del área Cerro Lila-Peine, Región de Antofagasta. Servicio Nacional de Geología y Mineria. *Carta Geológica de Chile, Serie Geología Básica*, 147. 1 mapa escala 1:100.000. Santiago, Chile.

NOBLET, C., LAVENU, A. & MAROCCO, R. (1996) Concept of continuum as opposed to periodic tectonism in the Andes. *Tectonophysics*, 255, 65-78.

OLIVEROS, V., FÉRAUD, G., AGUIRRE, L., FORNARI, M. & MORATA, D. (2006) The Early Andean Magmatic Province (EAMP): $^{40}Ar/^{39}Ar$ dating on Mesozoic volcanic and plutonic rocks from the Coastal Cordillera, northern Chile. *Journal of Volcanology and Geothermal Research*, 157, 311-330.

PANANONT, P., MPODOZIS, C., BLANCO, N., JORDAN, T.E. & BROWN, L.D. (2004) Cenozoic evolution of the northwestern Salar de Atacama Basin, northern Chile. *Tectonics*, 23, TC6007, doi: 10.1029/2003TC001595.

PARADA, M.A., FÉRAUD, G., FUENTES, F., AGUIRRE, L., MORATA, D. & LARRONDO, P. (2005) Ages and cooling history of the Early Cretaceous Caleu pluton: testimony of a switch from a rifted to a compressional continental margin in central Chile. *Journal of the Geological Society of London*, 162, 273-287.

PICHOWIAK, S., BUCHELT, M. & DAMM, K.W. (1990) Magmatic activity and tectonic setting of the early stages of the Andean cycle in northern Chile. *Geological Society of America Special Papers*, 241, 127-144. doi: 10.1130/SPE241-p127

RACZYNSKI, A. (1963) Geología del distrito minero de Tuina. *BSc. Thesis, Universidad de Chile,* (unpublished), p. 117. Santiago, Chile.

RAMÍREZ, C.F. & GARDEWEG, M. (1982) Hoja Toconao. *Carta Geológica de Chile,* 54, 1-122. 1 mapa escala 1:250.000. Santiago, Chile.

RAMOS, V.A. (2008) The Basement of the Central Andes: The Arequipa and Related Terranes. *Annual Review of Earth and Planetary Sciences,* 36, 289-324.

RAMOS, V.A. (2010) The tectonic regime along the Andes: Present-day and Mesozoic regimes. *Geological Journal,* 45, 2-25.

REUTTER, K.J., CHARRIER, R., GÖTZE, H.J., SCHURR, B., WIGGER, P., SCHEUBER, E., GIESE, P., REUTHER, C.D., SCHMIDT, S., RIETBROCK, A., CHONG, G. & BELMONTE-POOL, A. (2006) The Salar de Atacama Basin: a Subsiding Block within the Western Edge of the Altiplano-Puna Plateau. In *The Andes Active Subduction Orogeny* (Ed. by O. Oncken), pp. 303-325. Springer, Berlin.

SALFITY, J.A., MARQUILLAS, R.A., GARDEWEG, M.C., RAMÍREZ, C.F. & DAVIDSON, J. (1985) Correlaciones en el Cretácico superior del norte de la Argentina y Chile. In *Congreso Geológico Chileno No. 4 Actas,* 1, 654-667. Antofagasta.

SALFITY, J.A. & MARQUILLAS, R.A. (1999) La Cuenca Cretácica-terciaria del Norte Argentino. In *Geología Argentina, Servicio Geológico Minero, Anales 29* (Ed. by R. Caminos), pp. 613-626. Buenos Aires.SELLWOOD, B.W. & VALDES, P.J. (2006) Mesozoic climates: General circulation models and the rock record. *Sedimentary Geology*, 190, 269-287.

SERVICIO NACIONAL DE GEOLOGÍA Y MINERÍA. (2003) Mapa Geológico de Chile. 1 mapa escala 1:1.000.000. Santiago, Chile.

SIKS, B. & HORTON, B.K. (2011) Growth and fragmentation of the Andean foreland basin during eastward advance of fold-thrust deformation, Puna plateau and Eastern Cordillera, northern Argentina. *Tectonics*: doi:10.1029/2011TC002944, in press.

SKARMETA, J. (1983) The structural geology of the Sierra de Moreno, northern Chile. *Thesis, University of London,* (unpublished).

SOMOZA, R., TOMLINSON, A.J., CAFFE, P.J. & VILAS, J.F. (2012) Paleomagnetic evidence of earliest Paleocene deformation in Calama (~22°S), northern Chile: Andean-type or ridge-collision tectonics? *Journal of South American Earth Sciences*, 37, 208-213.

SOLA, A.M., BECCHIO, R.A. & PIMENTEL, M.M. (2013) Petrogenesis of migmatites and leucogranites from Sierra de Molinos, Salta, Northwest Argentina: A petrologic and geochemical study. *Lithos,* 177, 470-491.

SOLARI, L.A., GÓMEZ-TUENA, A., BERNAL, J.P., PÉREZ-ARVIZU, O. & TANNER, M. (2010) U-Pb zircon geochronology by an integrated LA-ICPMS microanalytical workstation: achievements in precision and accuracy. *Geostandards and Geoanalytical Research,* 34-1, 5-18.

STEINMAN, G. (1929) Geologie von Peru. Karl Winters Universitats-Buchhandlung, Heidelberg, p.448.

TOMLINSON, A.J., BLANCO, N., MAKSAEV, V., DILLES, J., GRUNDER, A.L. & LADINO, M. (2001) Geología de la Precordillera Andina de Quebrada Blanca-Chuquicamata, Regiones I y II (20°30'-22°30'S). *Servicio Nacional de Geología y Minería, Informe Registrado,* IR-01-20, 1-444. Santiago, Chile.

TUNIK, M., FOLGUERA, A., NAIPAUER, M., PIMENTEL, M. & RAMOS, V.A. (2010) Early uplift and orogenic deformation in the Neuquén Basin: Constraints on the Andean uplift from U-Pb and Hf isotopic data of detrital zircons. *Tectonophysics,* 489, 258-273.

WELTJE, G.J. (2002) Quantitative analysis of detrital modes: statistically rigorous confidence regions in ternary diagrams and their use in sedimentary petrology. *Earth-Science Reviews,* 57, 211-253.

WELTJE, G.J. (2006) Ternary sandstone composition and provenance: an evaluation of the 'Dickinson model'. *Geological Society, London, Special Publications,* 264, 79-99.

YANG, Y. & MIALL, A.D. (2010) Migration and stratigraphic fill of an underfilled foreland basin: Middle-Late Cenomanian Belle Fourche Formation in southern Alberta. *Sedimentary Geology,* 227, 51-64.

YANG, Y. (2011) Tectonically-driven underfilled-overfilled cycles, the middle Cretaceous in the northern Cordilleran foreland basin. *Sedimentary Geology,* 233, 15-27.

YUAN, X., SOBOLEV, S. & KIND, R. (2002) Moho topography in the central Andes and its geodynamic implications. *Earth Planetary Science Letters,* 199, 389–402.

ZAHID, K.M. & BARBEAU, D.L. (2011) Constructing sandstone provenance and classification ternary diagrams using electronic spreadsheet. *Journal of Sedimentary Research,* 81, 702-707.

ZIMMERMANN, U., NIEMEYER, H. & MEFFRE, S. (2009) Revealing the continental margin of Gondwana: The Ordovician arc of the Cordón de Lila (northern Chile). *International Journal of Earth Sciences*: doi: 10.1007/s00531-009-0483-811,

Table 1.

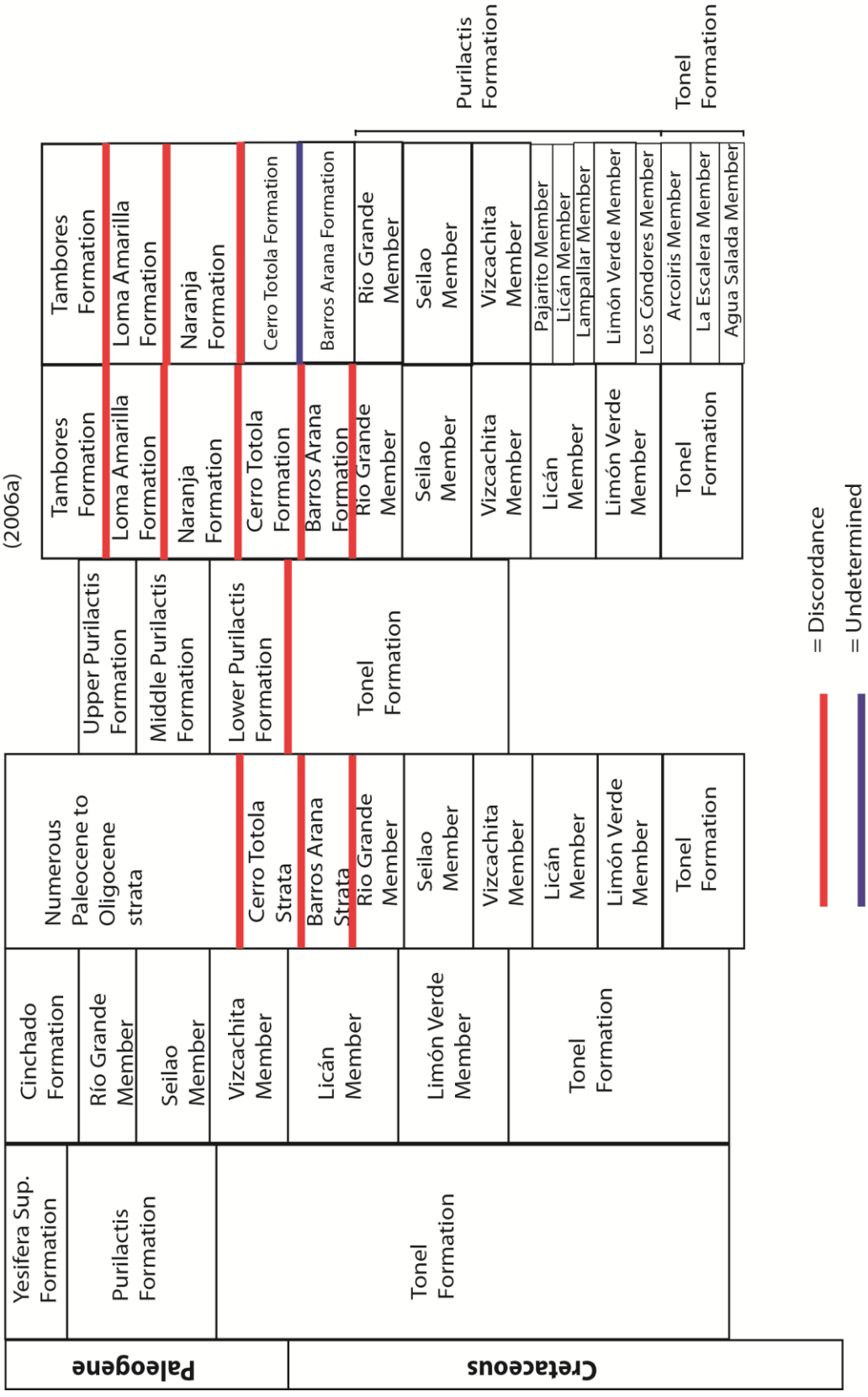

Table 2.

Litho-facies	Description	Interpretation
Sh	Medium- to fine-grained sandstones with horizontal lamination	Subcritical to supercritical flow transition.
Sp	Fine- to very fine- grained sandstones with planar cross lamination	2-D dune migration under lower regime conditions.
Sl	Medium- to very coarse-grained sandstones with low angle (<10°) cross-bedding	Deposition over inclined surfaces, or low-angle dune migration.
St	Medium- to coarse-grained sandstones with trough cross-bedding	3-D dune migration under lower regime conditions.
Gmm	Matrix-supported, massive, structureless conglomerate	Plastic, high-strength debris flow.
Gmg	Matrix-supported conglomerate, with inverse or normal grading	Pseudoplastic, low-strength debris flow.
Gch	Clast-supported conglomerate with stratification and/or local imbrication	Rapid downstream gravel transport; longitudinal bedforms.
Gcm	Clast-supported, massive, structureless conglomerate	Pseudplastic debris flows; hyper-concentrated flows.
Gpt	Clast-supported conglomerates with planar stratification	Slow downstream gravel transport; transverse bedforms.
Fm	Mud and silt with dessication marks and small scale ripples	Deposition from suspension and/or weak traction currents and dessication.

Table 3

Symbol	Description
Qm	Monocrystalline quartz
Qp	Polycrystalline quartz
Qt	Total quartz (Qp+Qm+Ch)
K	Potassium feldspar
P	Plagioclase
(PinLV)	(Plagioclase in volcanic fragments)
Ch	Chert
C	Carbonate
Sm	Sandstone/siltstone fragment
Ls	Total sedimentary fragments (Sm+C)
Lm	Metamorphic fragment
Lv	Volcanic fragment
Lt	Total lithic fragments (Lv+Lt+Lm+Ls)
M	Matrix and cement
D	Iron oxides and accessory minerals
Hb	Hornblende
Ol	Olivine

Figure 1.

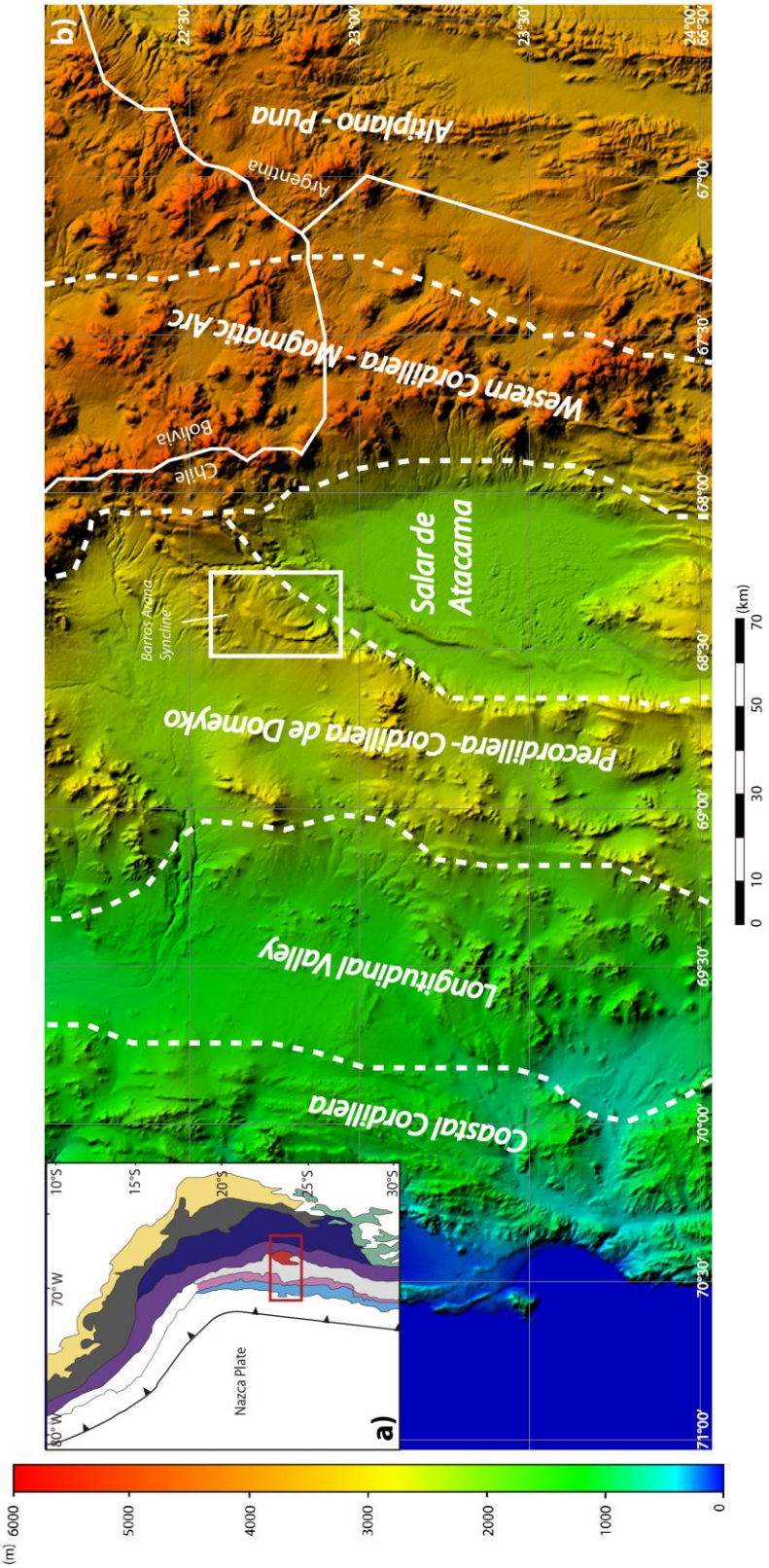

Figure 2.

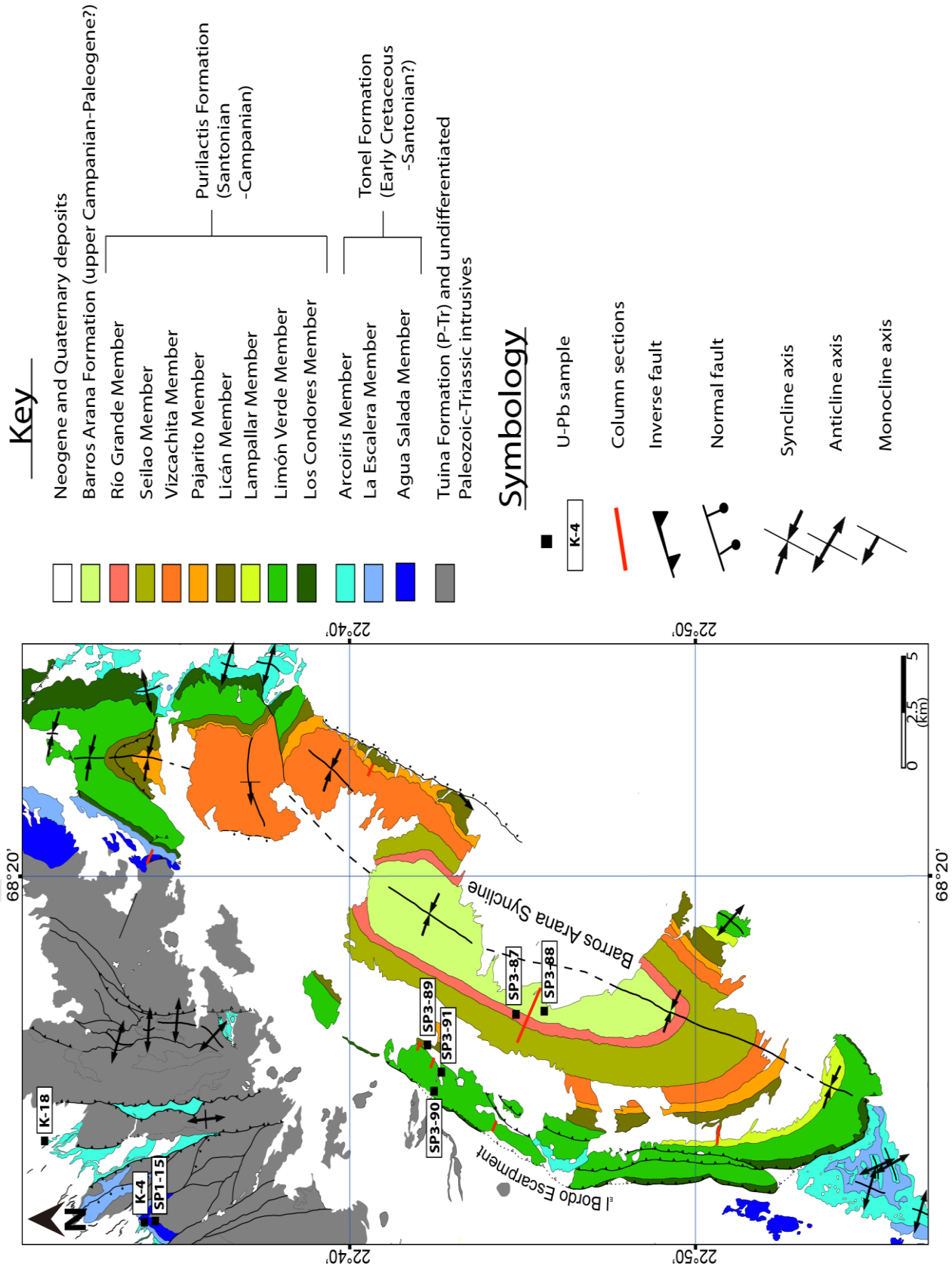

Figure 3.

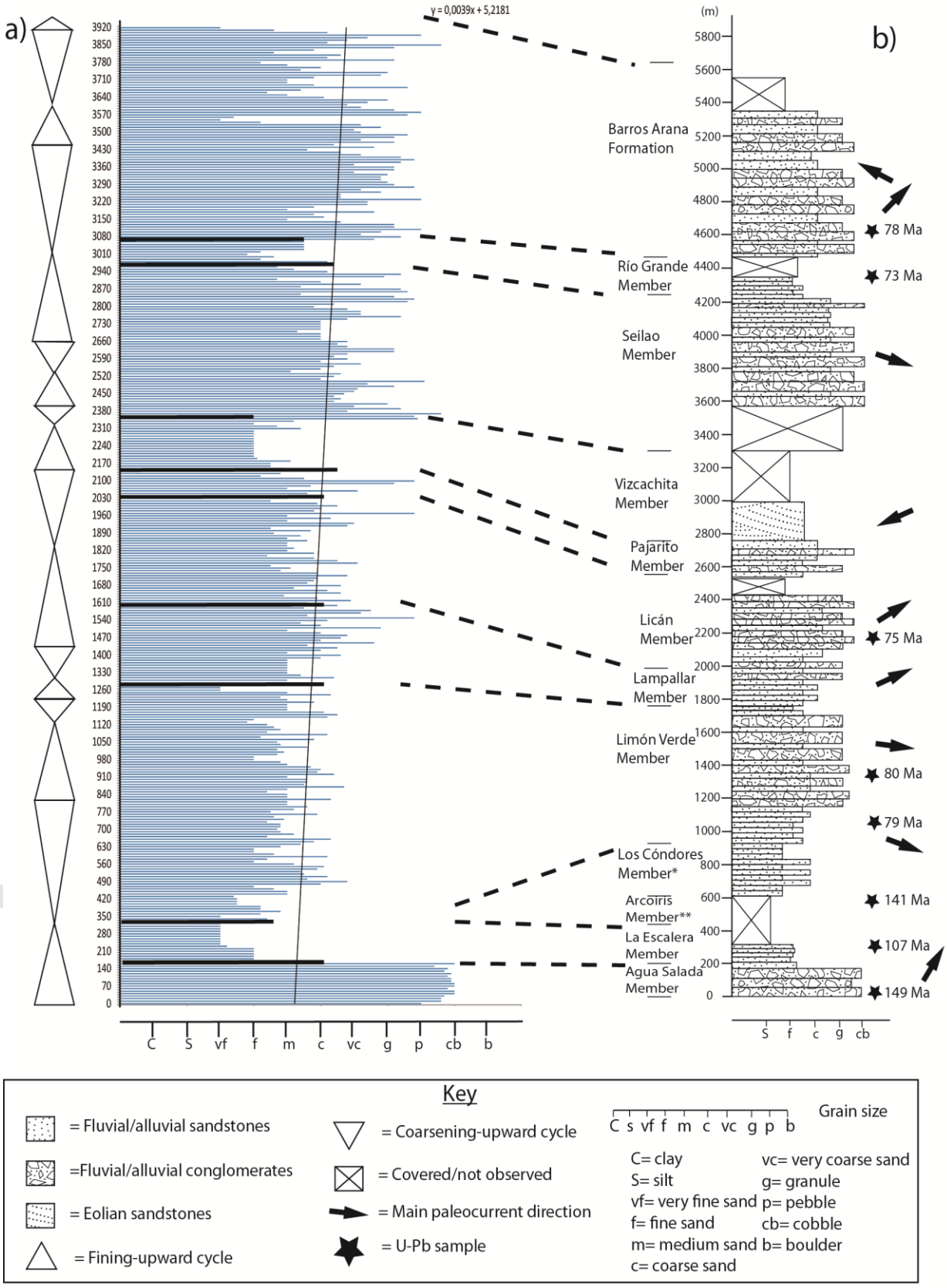

Figure 4.

Figure 5.

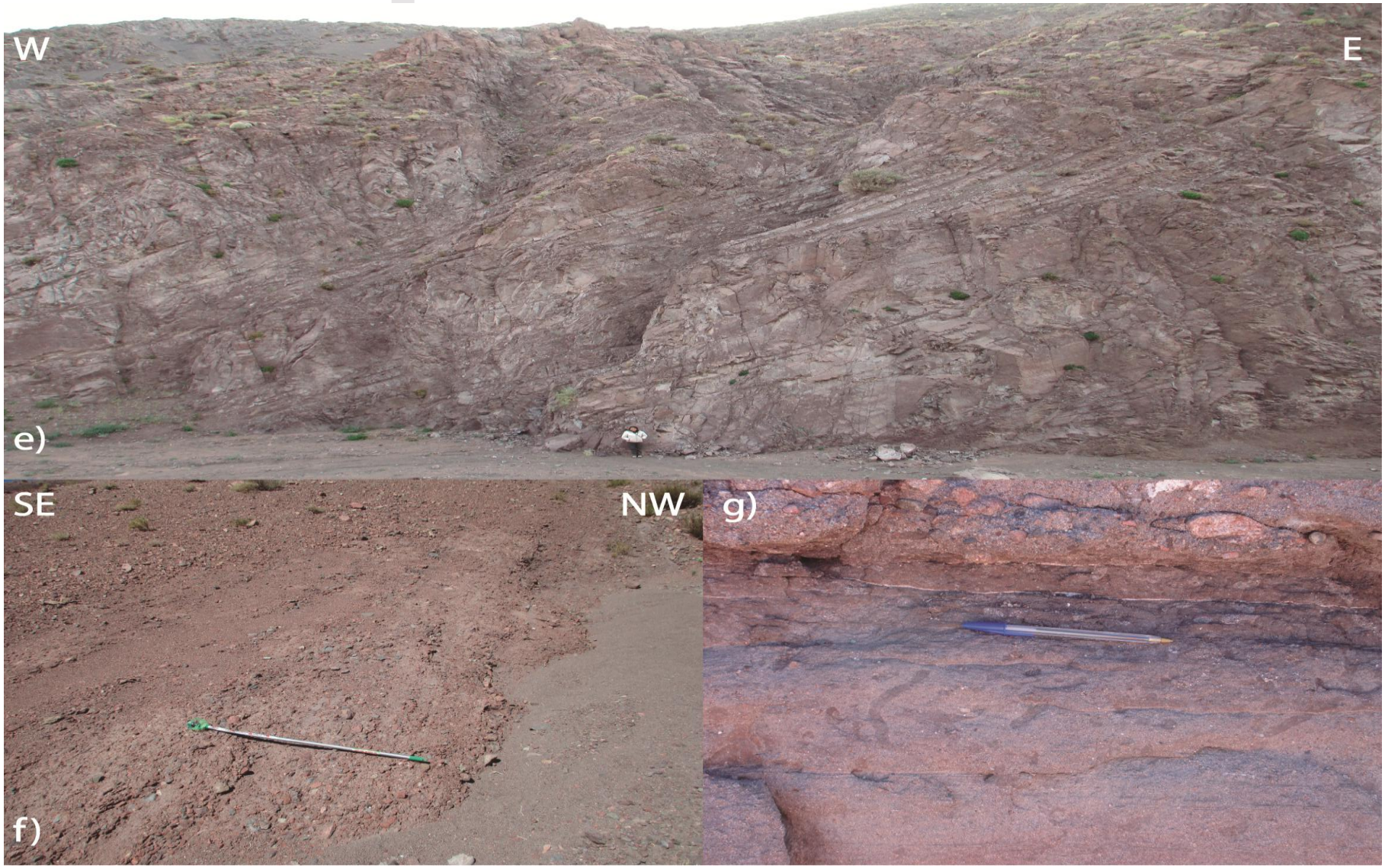

Figure 6.

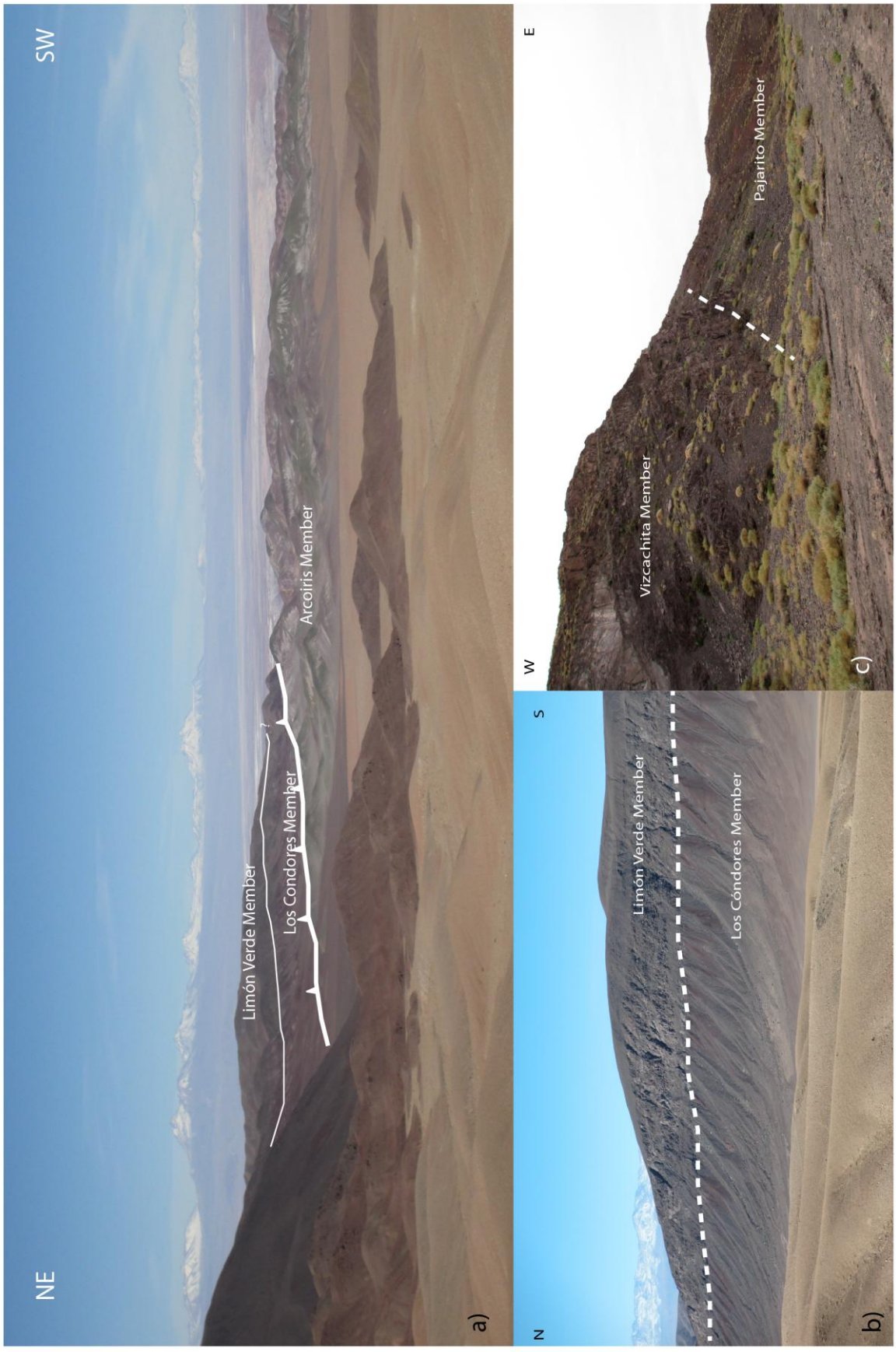

Figure 7.

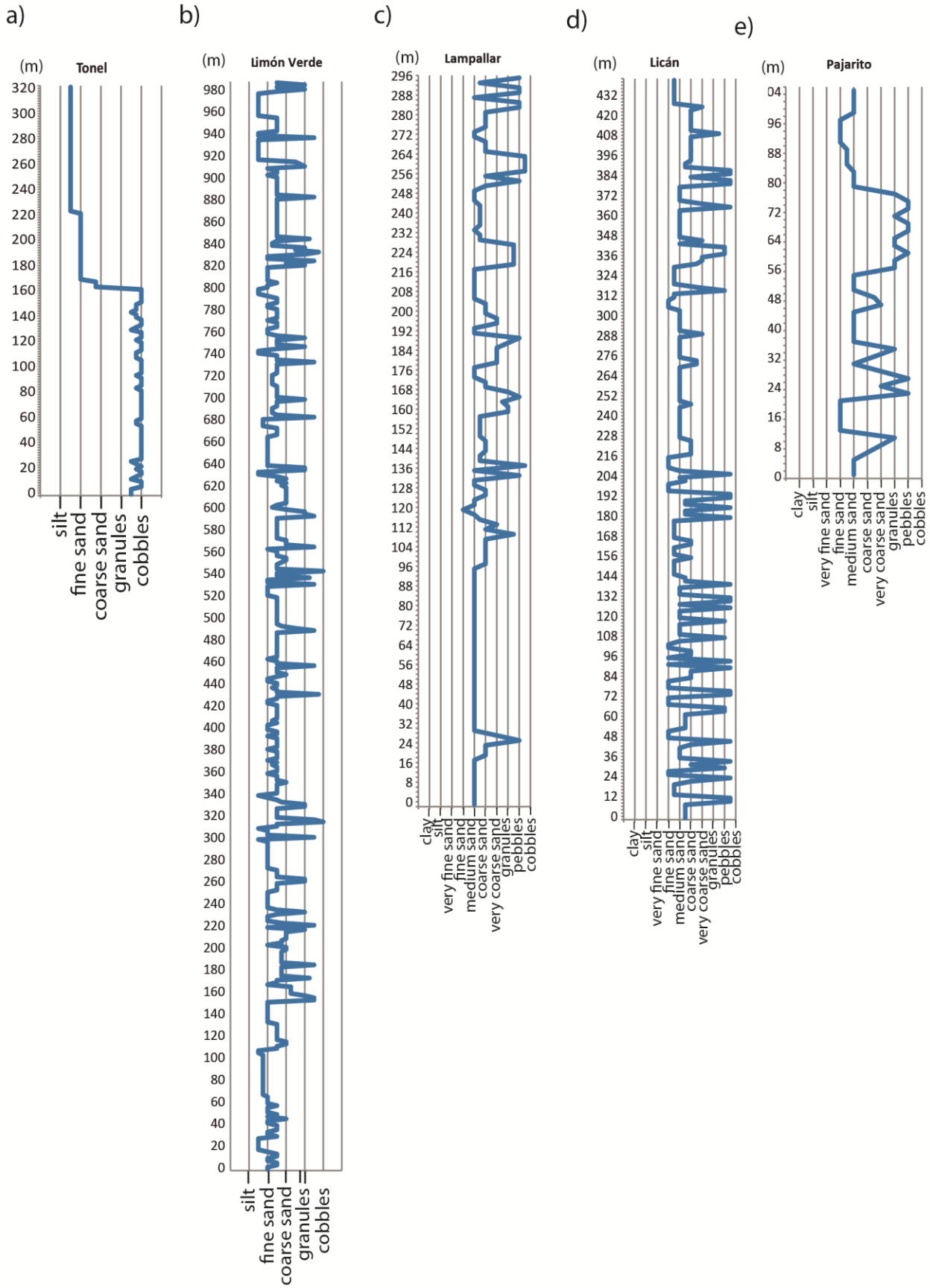

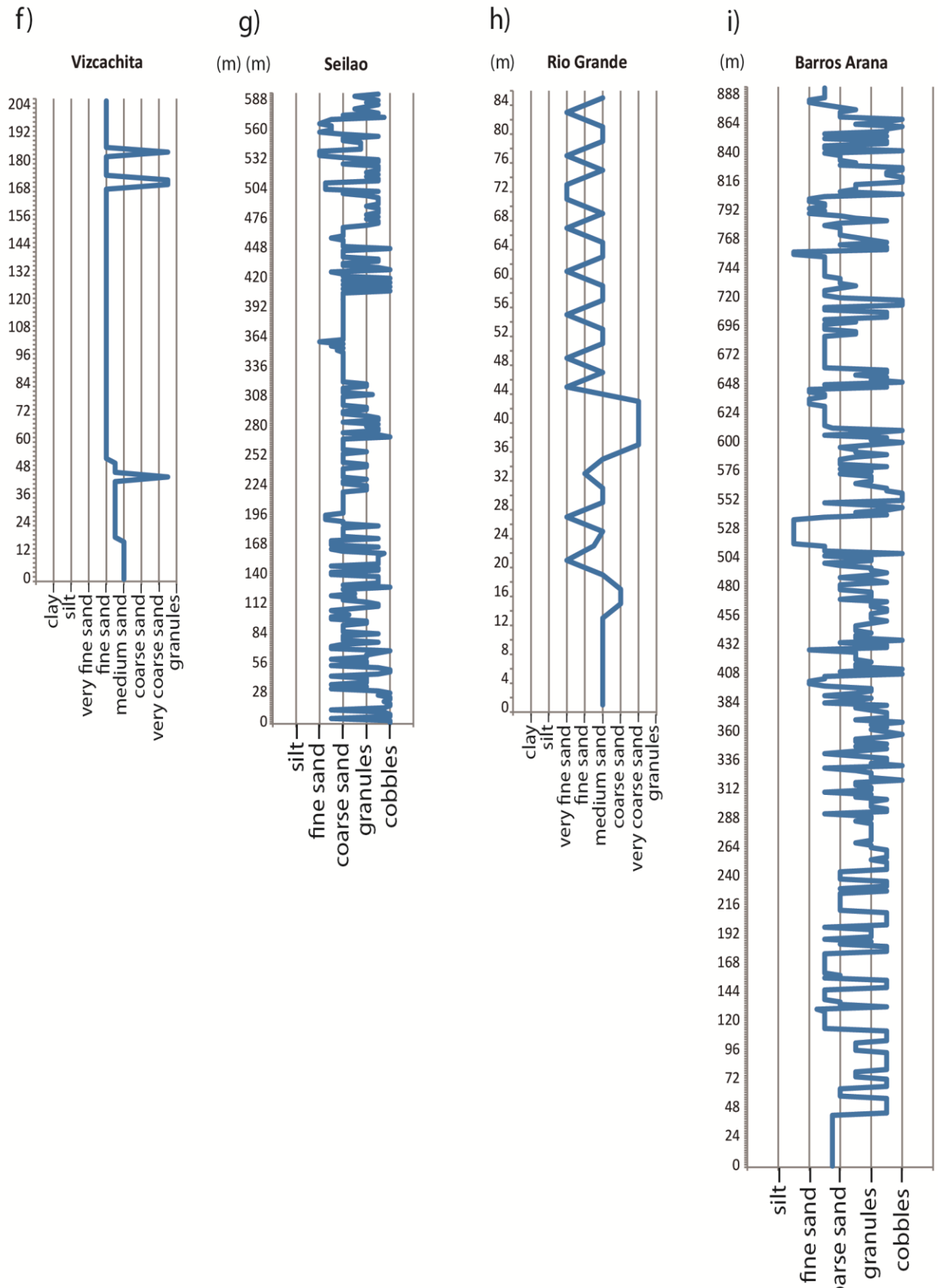

Figure 8.

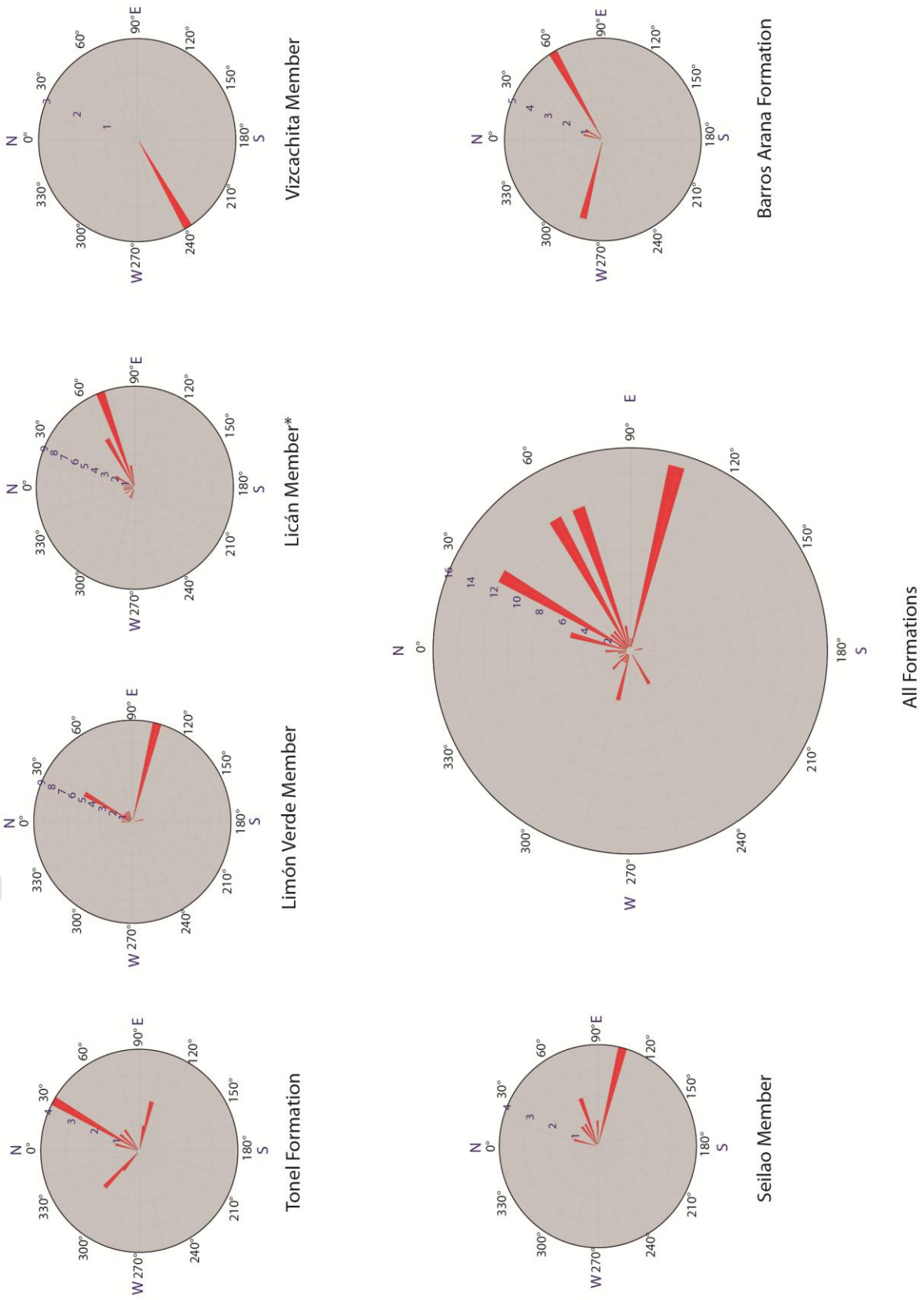

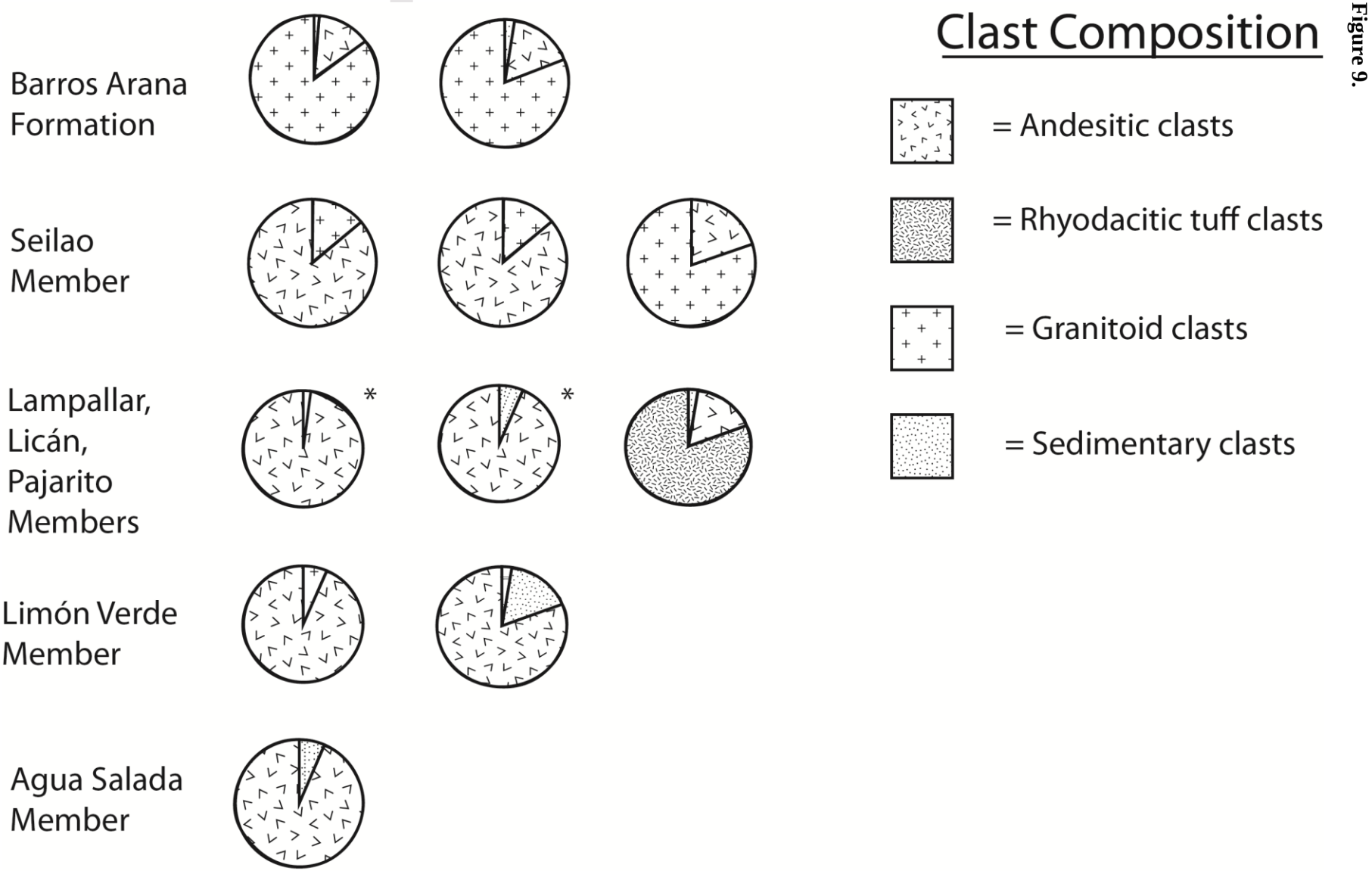

Figure 9.

Figure 10.

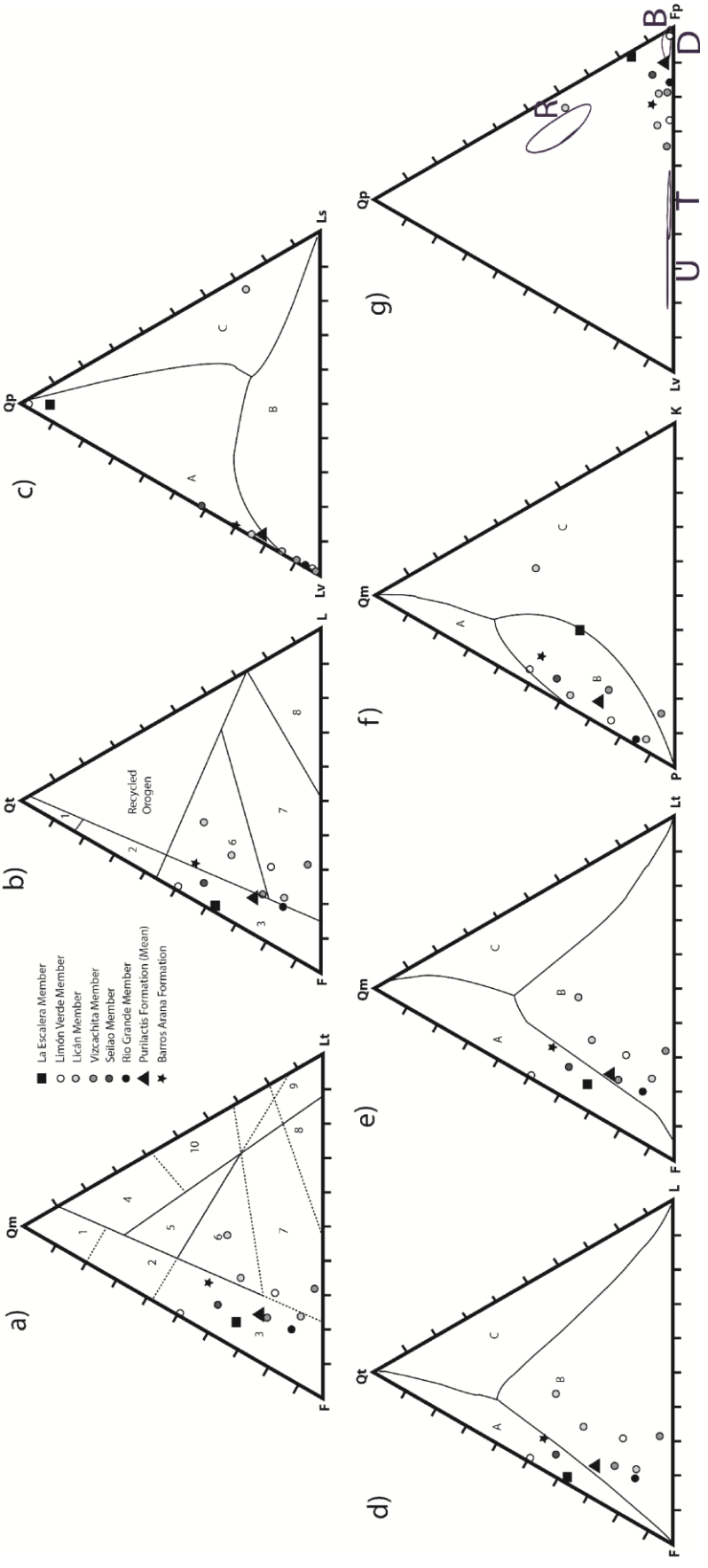

Figure 11.

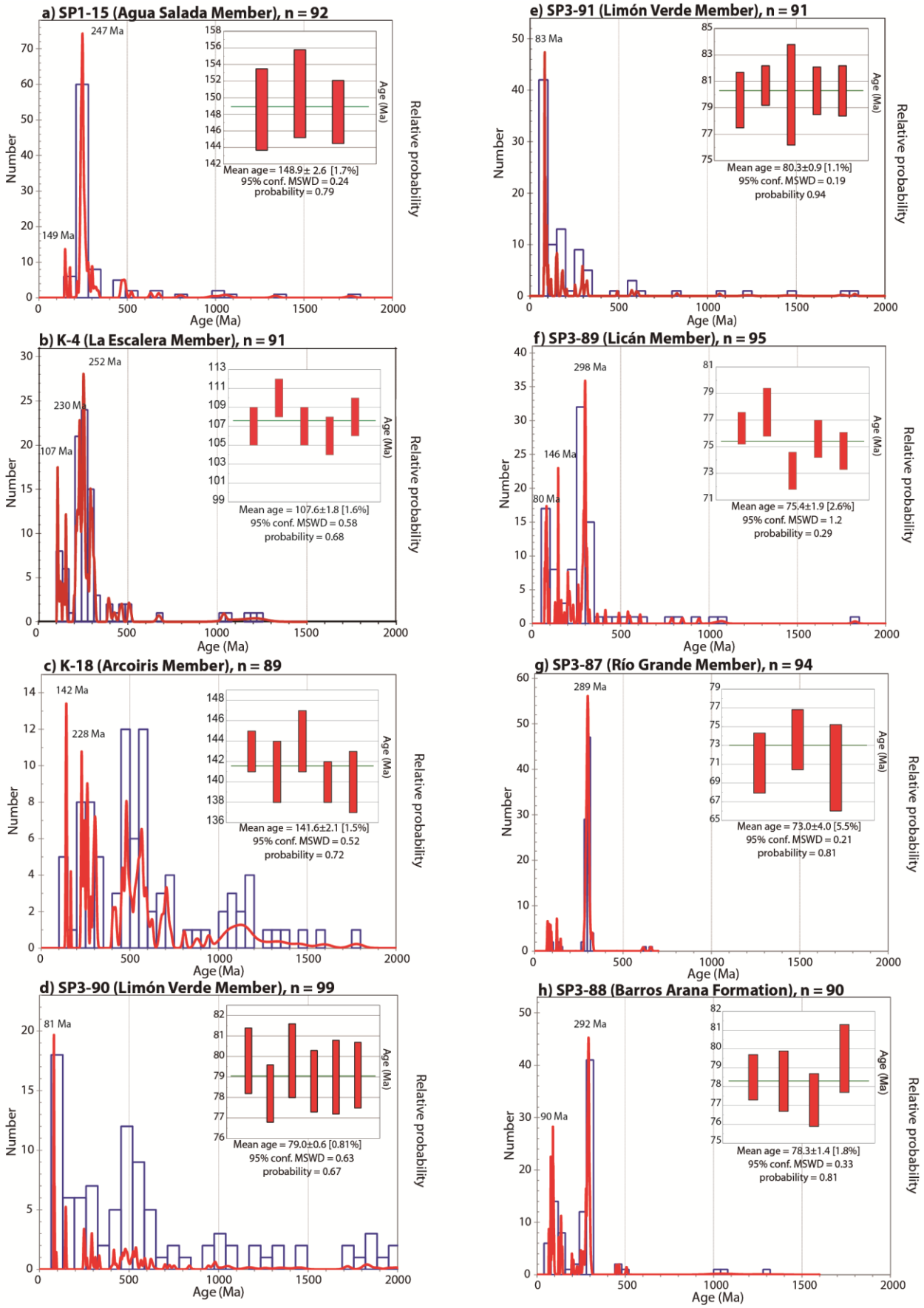

Figure 12.

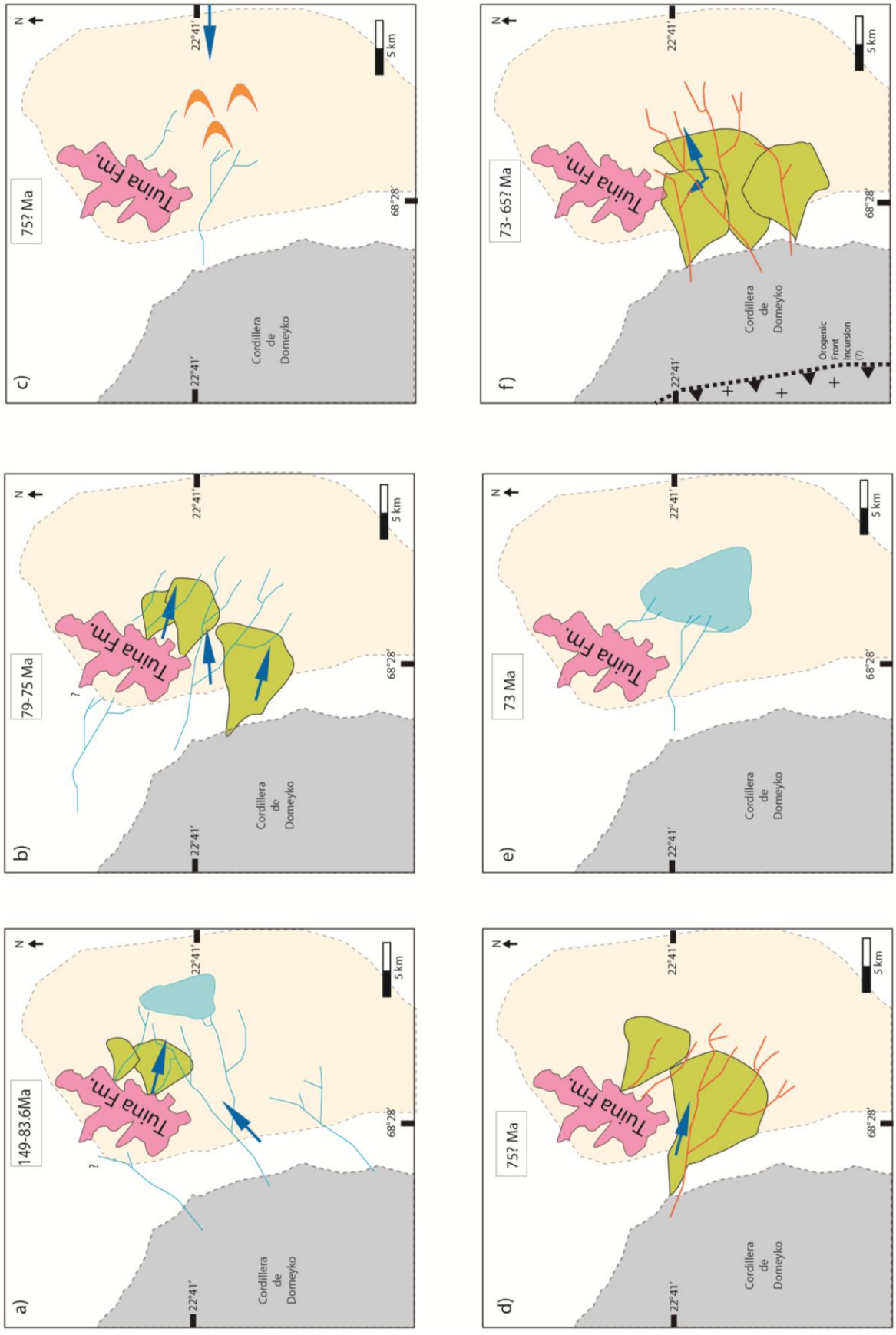

Figure 13.

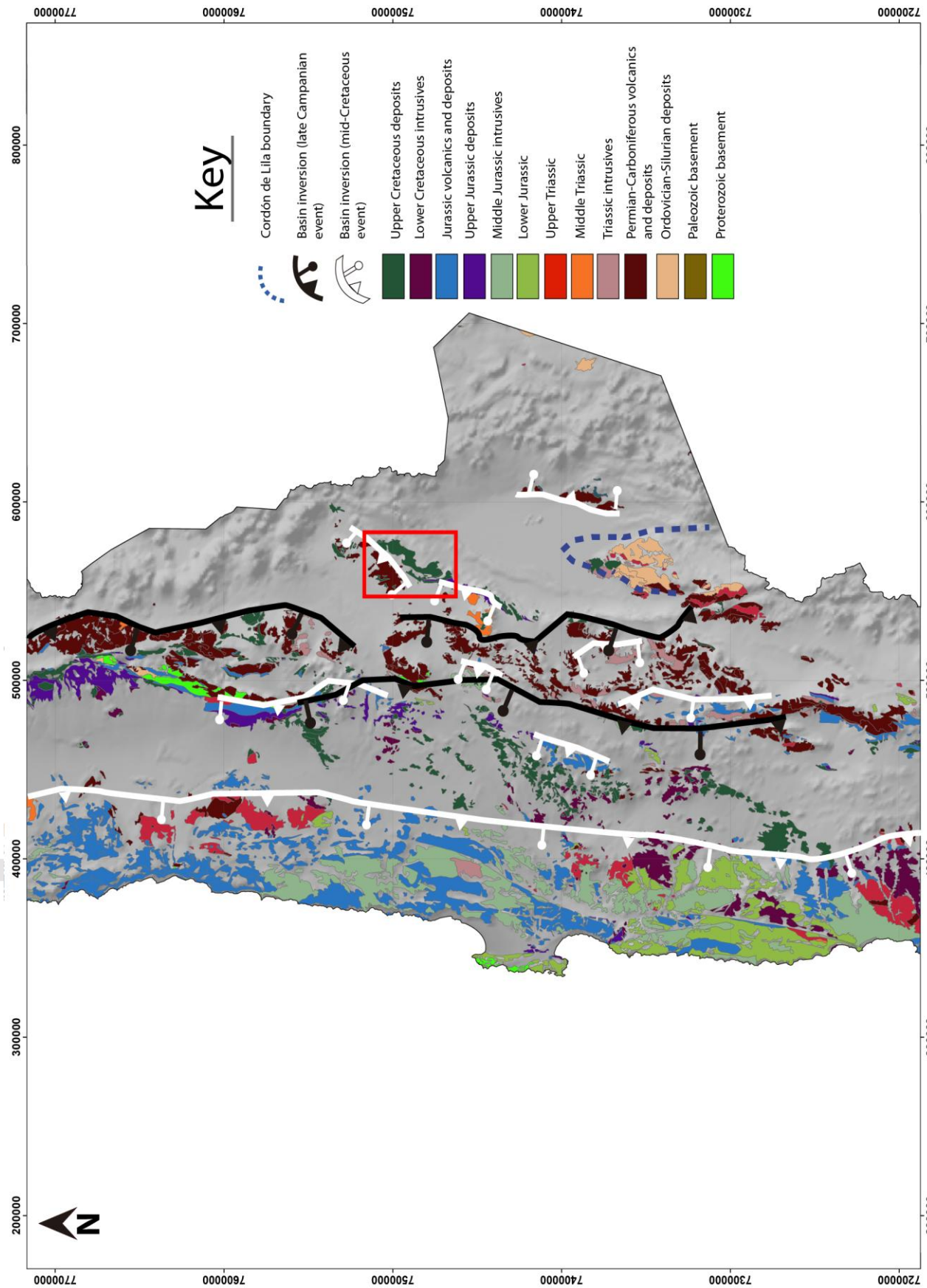

Figure 14.